

NUCLEAR MAGNETIC RESONANCE SPECTROSCOPY

Part Two: Carbon-13 Spectra, Including Heteronuclear Coupling with Other Nuclei

The study of carbon nuclei through nuclear magnetic resonance (NMR) spectroscopy is an important technique for determining the structures of organic molecules. Using it together with proton NMR and infrared spectroscopy, organic chemists can often determine the complete structure of an unknown compound without “getting their hands dirty” in the laboratory! Modern Fourier transform–NMR (FT-NMR) instrumentation makes it possible to obtain routine carbon spectra easily.

Carbon spectra can be used to determine the number of nonequivalent carbons and to identify the types of carbon atoms (methyl, methylene, aromatic, carbonyl, and so on) that may be present in a compound. Thus, carbon NMR provides direct information about the carbon skeleton of a molecule. Some of the principles of proton NMR apply to the study of carbon NMR; however, structural determination is generally easier with carbon-13 NMR spectra than with proton NMR. Typically, both techniques are used together to determine the structure of an unknown compound.

4.1 THE CARBON-13 NUCLEUS

Carbon-12, the most abundant isotope of carbon, is NMR inactive since it has a spin of zero (see Section 3.1). Carbon-13, or ^{13}C , however, has odd mass and does have nuclear spin, with $I = \frac{1}{2}$. Unfortunately, the resonances of ^{13}C nuclei are more difficult to observe than those of protons (^1H). They are about 6000 times weaker than proton resonances, for two major reasons.

First, the natural abundance of carbon-13 is very low; only 1.08% of all carbon atoms in nature are ^{13}C atoms. If the total number of carbons in a molecule is low, it is very likely that a majority of the molecules in a sample will have no ^{13}C nuclei at all. In molecules containing a ^{13}C isotope, it is unlikely that a second atom in the same molecule will be a ^{13}C atom. Therefore, when we observe a ^{13}C spectrum, we are observing a spectrum built up from a collection of molecules, where each molecule supplies no more than a single ^{13}C resonance. No *single* molecule supplies a complete spectrum.

Second, since the magnetogyric ratio of a ^{13}C nucleus is smaller than that of hydrogen (Table 3.2), ^{13}C nuclei always have resonance at a frequency lower than protons. Recall that at lower frequencies, the population of excess nuclei is reduced (Table 3.3); this, in turn, reduces the sensitivity of NMR detection procedures.

Through the use of modern Fourier transform instrumentation (Section 3.7B), it is possible to obtain ^{13}C NMR spectra of organic compounds even though detection of carbon signals is difficult compared to detection of proton spectra. To compensate for the low natural abundance of carbon, a greater number of individual scans of the spectrum must be accumulated than is common for a proton spectrum.

For a given magnetic field strength, the resonance frequency of a ^{13}C nucleus is about one-fourth the frequency required to observe proton resonances (see Table 3.2). For example, in a 7.05-Tesla applied magnetic field, protons are observed at 300 MHz while ^{13}C nuclei are observed at about 75 MHz. With modern instrumentation, it is a simple matter to switch the transmitter frequency from the value required to observe proton resonances to the value required for ^{13}C resonances.

4.2 CARBON-13 CHEMICAL SHIFTS

A. Correlation Charts

An important parameter derived from carbon-13 spectra is the chemical shift. The correlation chart in Figure 4.1 shows typical ^{13}C chemical shifts, listed in parts per million (ppm) from tetramethylsilane (TMS), where the carbons of the methyl groups of TMS (not the hydrogens) are used for reference. Approximate ^{13}C chemical shift ranges for selected types of carbon are also given in Table 4.1. Notice that the chemical shifts appear over a range (0 to 220 ppm) much larger than that observed for protons (0 to 12 ppm). Because of the very large range of values, nearly every nonequivalent carbon atom in an organic molecule gives rise to a peak with a different chemical shift. Peaks rarely overlap as they often do in proton NMR.

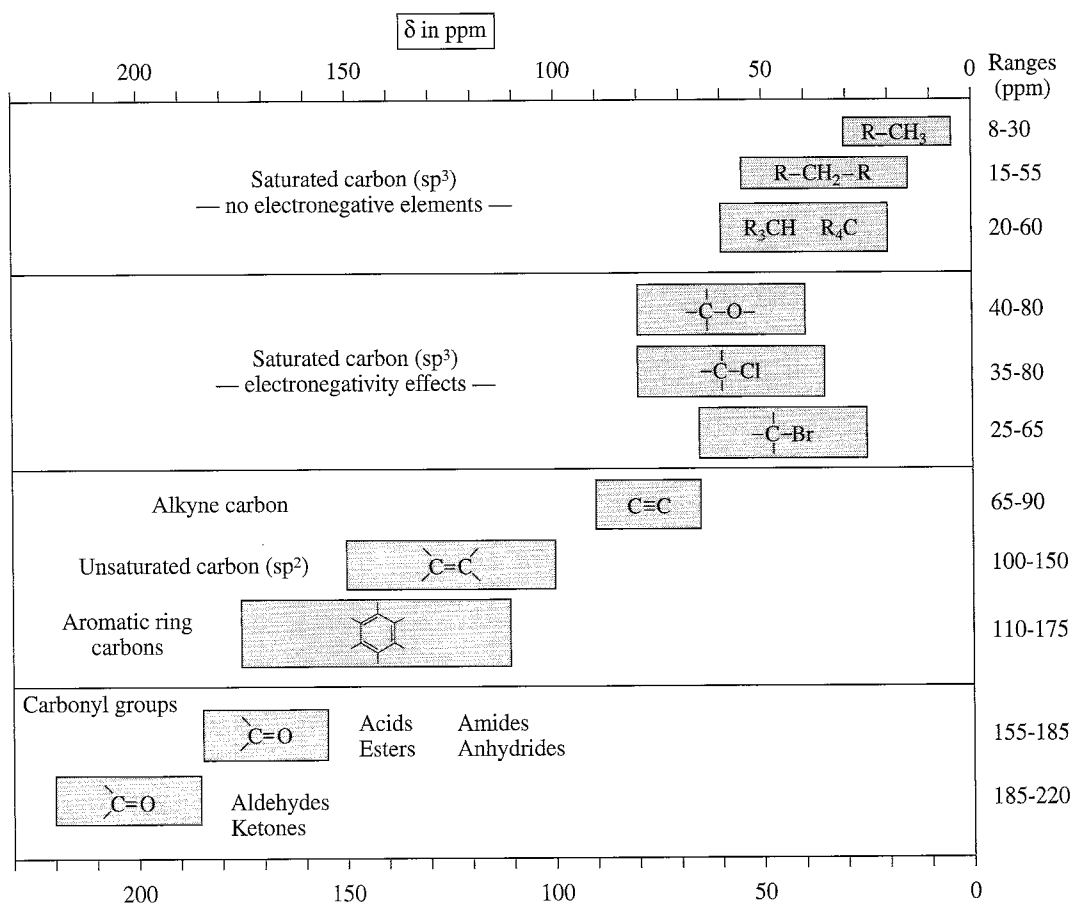
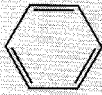

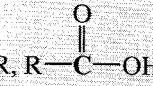


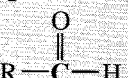


FIGURE 4.1 A correlation chart for ^{13}C chemical shifts (chemical shifts are listed in parts per million from TMS).

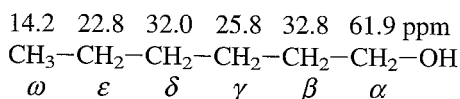
TABLE 4.1
APPROXIMATE ^{13}C CHEMICAL SHIFT RANGES (ppm) FOR SELECTED TYPES OF CARBON

$\text{R}-\text{CH}_3$	8-30		$\text{C}=\text{C}$	65-90
R_2CH_2	15-55		$\text{C}=\text{C}$	100-150
R_3CH	20-60		$\text{C}=\text{N}$	110-140
$\text{C}-\text{I}$	0-40			110-175
$\text{C}-\text{Br}$	25-65			
$\text{C}-\text{N}$	30-65			155-185
$\text{C}-\text{Cl}$	35-80			155-185
$\text{C}-\text{O}$	40-80			185-220

The correlation chart is divided into four sections. Saturated carbon atoms appear at highest field, nearest to TMS (8 to 60 ppm). The next section of the correlation chart demonstrates the effect of electronegative atoms (40 to 80 ppm). The third section of the chart includes alkene and aromatic ring carbon atoms (100 to 175 ppm). Finally, the fourth section of the chart contains carbonyl carbons, which appear at the lowest field values (155 to 220 ppm).

Electronegativity, hybridization, and anisotropy all affect ^{13}C chemical shifts in nearly the same fashion as they affect ^1H chemical shifts; however ^{13}C chemical shifts are about 20 times larger¹. Electronegativity (Section 3.11A) produces the same deshielding effect in carbon NMR as in proton NMR—the electronegative element produces a large downfield shift. The shift is greater for a ^{13}C atom than for a proton since the electronegative atom is directly attached to the ^{13}C atom, and the effect occurs through only a single bond, $\text{C}-\text{X}$. With protons, the electronegative atoms are attached to carbon, not hydrogen; the effect occurs through two bonds, $\text{H}-\text{C}-\text{X}$, rather than one.

In ^1H NMR, the effect of an electronegative element on chemical shift diminishes with distance, but it is always in the same direction (deshielding and downfield). In ^{13}C NMR, an electronegative element also causes a downfield shift in the α and β carbons, but it usually leads to a small *upfield* shift for the γ carbon. This effect is clearly seen in the carbons of hexanol:



The shift for C3, the γ carbon, seems quite at odds with the expected effect of an electronegative substituent. This anomaly points up the need to consult detailed correlation tables for ^{13}C chemical shifts. Such tables appear in Appendix 7 and are discussed in the next section.

¹This is sometimes called the *20x Rule*. See Macomber, R., "Proton-Carbon Chemical Shift Correlations," *Journal of Chemical Education*, 68(a), 284-5, 1991.

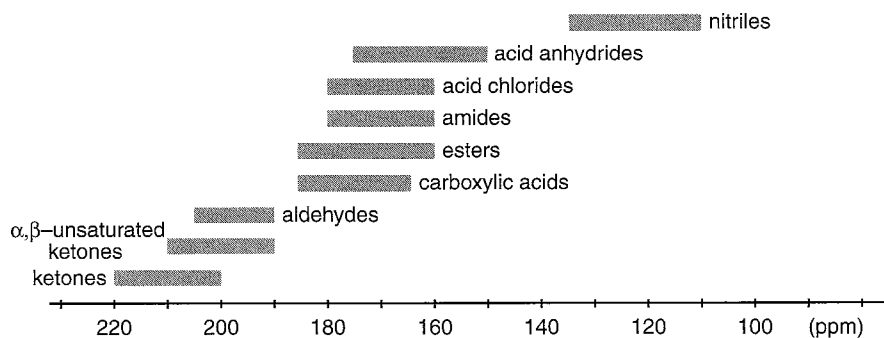


FIGURE 4.2 A ^{13}C correlation chart for carbonyl and nitrile functional groups.

Analogous with ^1H shifts, changes in hybridization (Section 3.11B) also produce larger shifts for the carbon-13 that is *directly involved* (no bonds) than they do for the hydrogens attached to that carbon (one bond). In ^{13}C NMR, the carbons of carbonyl groups have the largest chemical shifts, due both to sp^2 hybridization and to the fact that an electronegative oxygen is directly attached to the carbonyl carbon, deshielding it even further. Anisotropy (Section 3.12) is responsible for the large chemical shifts of the carbons in aromatic rings and alkenes.

Notice that the range of chemical shifts is larger for carbon atoms than for hydrogen atoms. Because the factors affecting carbon shifts operate either through one bond or directly on carbon, they are greater than those for hydrogen, which operate through more bonds. As a result, the entire range of chemical shifts becomes larger for ^{13}C (0 to 220 ppm) than for ^1H (0 to 12 ppm).

Many of the important functional groups of organic chemistry contain a carbonyl group. In determining the structure of a compound containing a carbonyl group, it is frequently helpful to have some idea of the type of carbonyl group in the unknown. Figure 4.2 illustrates the typical ranges of ^{13}C chemical shifts for some carbonyl-containing functional groups. Although there is some overlap in the ranges, ketones and aldehydes are easy to distinguish from the other types. Chemical shift data for carbonyl carbons are particularly powerful when combined with data from an infrared spectrum.

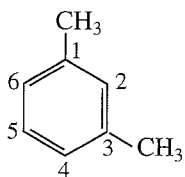
B. Calculation of ^{13}C Chemical Shifts

Nuclear magnetic resonance spectroscopists have accumulated, organized, and tabulated a great deal of data for ^{13}C chemical shifts. It is possible to predict the chemical shift of almost any ^{13}C atom from these tables, starting with a base value for the molecular skeleton and then adding increments that correct the value for each substituent. Corrections for the substituents depend on both the type of substituent and its position relative to the carbon atom being considered. Corrections for rings are different from those for chains, and they frequently depend on stereochemistry.

Consider *m*-xylene (1,3-dimethylbenzene) as an example. Consulting the tables, you will find that the base value for the carbons in a benzene ring is 128.5 ppm. Next, look in the substituent tables that relate to benzene rings for the methyl substituent corrections (Table A8.7). These values are

	<i>ipso</i>	<i>ortho</i>	<i>meta</i>	<i>para</i>
CH_3 :	9.3	0.7	-0.1	-2.9 ppm

The *ipso* carbon is the one to which the substituent is directly attached. The calculations for *m*-xylene start with the base value and add these increments as follows:



$$\text{C1} = \text{base} + \textit{ipso} + \textit{meta} = 128.5 + 9.3 + (-0.1) = 137.3 \text{ ppm}$$

$$\text{C2} = \text{base} + \textit{ortho} + \textit{ortho} = 128.5 + 0.7 + 0.7 = 129.9 \text{ ppm}$$

$$\text{C3} = \text{C1}$$

$$\text{C4} = \text{base} + \textit{ortho} + \textit{para} = 128.5 + 0.7 + (-2.9) = 126.3 \text{ ppm}$$

$$\text{C5} = \text{base} + \textit{meta} + \textit{meta} = 128.5 + 2(-0.1) = 128.3 \text{ ppm}$$

$$\text{C6} = \text{C4}$$

The observed values for C1, C2, C4, and C5 of *m*-xylene are 137.6, 130.0, 126.2, and 128.2 ppm, respectively, and the calculated values agree well with those actually measured.

Appendix 8 presents some ^{13}C chemical shift correlation tables with instructions. Complete ^{13}C chemical shift correlation tables are too numerous to include in this book. If you are interested, consult the textbooks by Levy, Macomber, Silverstein, and Friebolin, which are listed in the references at the end of this chapter. Even more convenient than tables are computer programs that calculate ^{13}C chemical shifts. In the more advanced programs, the operator need only sketch the molecule on the screen, using a mouse, and the program will calculate both the chemical shifts and the rough appearance of the spectrum. Some of these programs are also listed in the references.

4.3 PROTON-COUPLED ^{13}C SPECTRA—SPIN-SPIN SPLITTING OF CARBON-13 SIGNALS

Unless a molecule is artificially enriched by synthesis, the probability of finding two ^{13}C atoms in the same molecule is low. The probability of finding two ^{13}C atoms adjacent to each other in the same molecule is even lower. Therefore, we rarely observe **homonuclear** (carbon–carbon) spin–spin splitting patterns where the interaction occurs between two ^{13}C atoms. However, the spins of protons attached directly to ^{13}C atoms do interact with the spin of carbon and cause the carbon signal to be split according to the $n + 1$ Rule. This is **heteronuclear** (carbon–hydrogen) coupling involving two different types of atoms. With ^{13}C NMR, we generally examine splitting that arises from the protons *directly attached* to the carbon atom being studied. This is a one-bond coupling. Remember that in proton NMR, the most common splittings are *homonuclear* (hydrogen–hydrogen) and occur between protons attached to *adjacent* carbon atoms. In these cases, the interaction is a three-bond coupling, H–C–C–H.

Figure 4.3 illustrates the effect of protons directly attached to a ^{13}C atom. The $n + 1$ Rule predicts the degree of splitting in each case. The resonance of a ^{13}C atom with three attached protons, for instance, is split into a quartet ($n + 1 = 3 + 1 = 4$). The possible spin combinations for the three protons are the same as those illustrated in Figure 3.33, and each spin combination interacts with carbon to give a different peak of the multiplet. Since the hydrogens are directly attached to the carbon-13 (one-bond couplings), the coupling constants for this interaction are quite large, with J values of about 100 to 250 Hz. Compare the typical three-bond H–C–C–H couplings that are common in NMR spectra, which have J values of about 1 to 20 Hz.

It is important to note while examining Figure 4.3 that you are not “seeing” protons directly when looking at a ^{13}C spectrum (proton resonances occur at frequencies outside the range used to obtain ^{13}C spectra); you are observing only the effect of the protons on ^{13}C atoms. Also, remember that we cannot observe ^{12}C , because it is NMR inactive.

Spectra that show the spin–spin splitting, or coupling, between carbon-13 and the protons directly attached to it are called **proton-coupled spectra** or sometimes **nondecoupled spectra** (see the next section). Figure 4.4a is the proton-coupled ^{13}C NMR spectrum of ethyl phenylacetate. In this spectrum, the first quartet downfield from TMS (14.2 ppm) corresponds to the carbon of the methyl group. It is split into a quartet ($J = 127$ Hz) by the three attached hydrogen atoms (^{13}C –H,

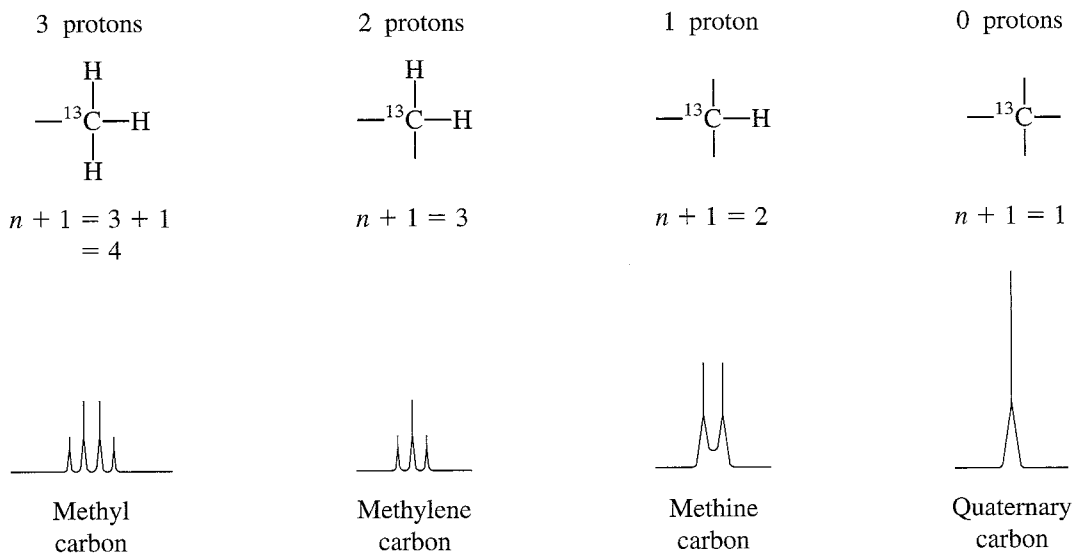


FIGURE 4.3 The effect of attached protons on ^{13}C resonances.

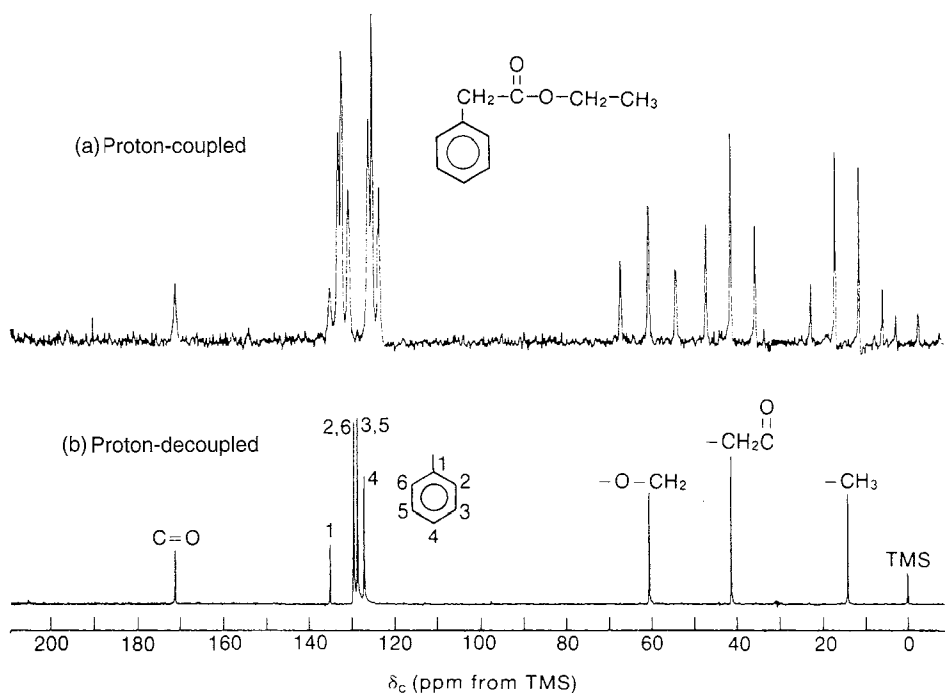


FIGURE 4.4 Ethyl phenylacetate. (a) The proton-coupled ^{13}C spectrum (20 MHz). (b) The proton-decoupled ^{13}C spectrum (20 MHz). (From Moore, J. A., and D. L. Dalrymple, *Experimental Methods in Organic Chemistry*, W. B. Saunders, Philadelphia, 1976.)

one-bond couplings). In addition, although it cannot be seen on the scale of this spectrum (an expansion must be used), each of the quartet lines is split into a closely spaced triplet ($J = \text{ca. } 1 \text{ Hz}$). This additional fine splitting is caused by the two protons on the adjacent $-\text{CH}_2-$ group. These are

two-bond couplings ($\text{H}-\text{C}-^{13}\text{C}$) of a type that occurs commonly in ^{13}C spectra, with coupling constants that are generally quite small ($J = 0-2$ Hz) for systems with carbon atoms in an aliphatic chain. Because of their small size, these couplings are frequently ignored in the routine analysis of spectra, with greater attention being given to the larger one-bond splittings seen in the quartet itself.

There are two $-\text{CH}_2-$ groups in ethyl phenylacetate. The one corresponding to the ethyl $-\text{CH}_2-$ group is found farther downfield (60.6 ppm), as this carbon is deshielded by the attached oxygen. It is a triplet because of the two attached hydrogens (one-bond couplings). Again, although it is not seen in this unexpanded spectrum, the three hydrogens on the adjacent methyl group finely split each of the triplet peaks into a quartet. The benzyl $-\text{CH}_2-$ carbon is the intermediate triplet (41.4 ppm). Farthest downfield is the carbonyl-group carbon (171.1 ppm). On the scale of this presentation it is a singlet (no directly attached hydrogens), but because of the adjacent benzyl $-\text{CH}_2-$ group, it is actually split finely into a triplet. The aromatic-ring carbons also appear in the spectrum, and they have resonances in the range from 127 to 136 ppm. Section 4.12 will discuss aromatic-ring ^{13}C resonances.

Proton-coupled spectra for large molecules are often difficult to interpret. The multiplets from different carbons commonly overlap because the $^{13}\text{C}-\text{H}$ coupling constants are frequently larger than the chemical shift differences of the carbons in the spectrum. Sometimes, even simple molecules such as ethyl phenylacetate (Fig. 4.4a) are difficult to interpret. Proton decoupling, which is discussed in the next section, avoids this problem.

4.4 PROTON-DECOUPLED ^{13}C SPECTRA

By far the great majority of ^{13}C NMR spectra are obtained as **proton-decoupled spectra**. The decoupling technique obliterates all interactions between protons and ^{13}C nuclei; therefore, only **singlets** are observed in a decoupled ^{13}C NMR spectrum. Although this technique simplifies the spectrum and avoids overlapping multiplets, it has the disadvantage that the information on attached hydrogens is lost.

Proton **decoupling** is accomplished in the process of determining a ^{13}C NMR spectrum by simultaneously irradiating all of the protons in the molecule with a broad spectrum of frequencies in the proper range. Most modern NMR spectrometers provide a second, tunable radiofrequency generator, the **decoupler**, for this purpose. Irradiation causes the protons to become saturated, and they undergo rapid upward and downward transitions, among all their possible spin states. These rapid transitions decouple any spin-spin interactions between the hydrogens and the ^{13}C nuclei being observed. In effect, all spin interactions are averaged to zero by the rapid changes. The carbon nucleus "senses" only one average spin state for the attached hydrogens rather than two or more distinct spin states.

Figure 4.4b is a proton-decoupled spectrum of ethyl phenylacetate. The proton-coupled spectrum (Fig. 4.4a) was discussed in Section 4.3. It is interesting to compare the two spectra to see how the proton decoupling technique simplifies the spectrum. Every chemically and magnetically distinct carbon gives only a single peak. Notice, however, that the two *ortho* ring carbons (carbons 2 and 6) and the two *meta* ring carbons (carbons 3 and 5) are equivalent by symmetry and that each gives only a single peak.

Figure 4.5 is a second example of a proton-decoupled spectrum. Notice that the spectrum shows three peaks, corresponding to the exact number of carbon atoms in 1-propanol. If there are no equivalent carbon atoms in a molecule, a ^{13}C peak will be observed for *each* carbon. Notice also that the assignments given in Figure 4.5 are consistent with the values in the chemical shift table (Fig. 4.1). The carbon atom closest to the electronegative oxygen is farthest downfield, and the methyl carbon is at highest field.

The three-peak pattern centered at $\delta = 77$ ppm is due to the solvent CDCl_3 . This pattern results from the coupling of a deuterium (^2H) nucleus to the ^{13}C nucleus (see Section 4.13). Often the CDCl_3 pattern is used as an internal reference, in place of TMS.

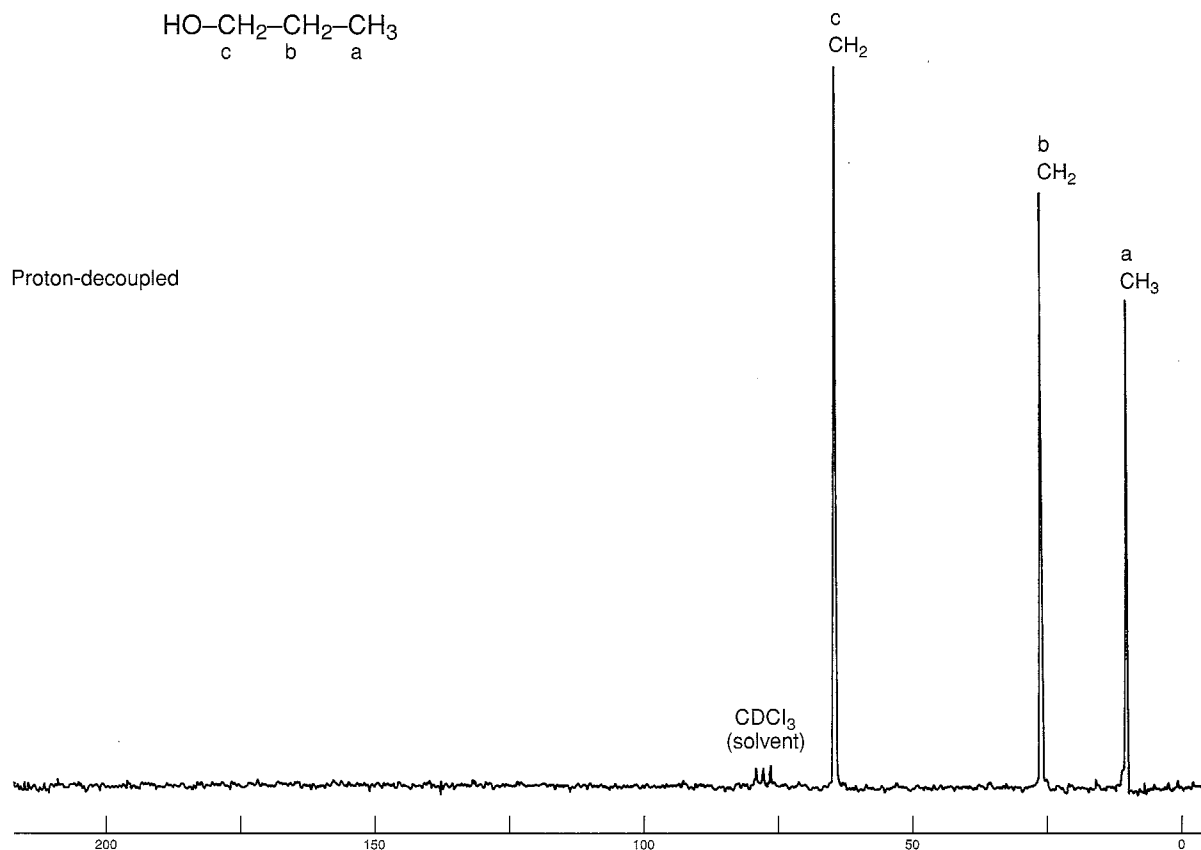


FIGURE 4.5 The proton-decoupled ^{13}C spectrum of 1-propanol (22.5 MHz).

4.5 NUCLEAR OVERHAUSER ENHANCEMENT (NOE)

When we obtain a proton-decoupled ^{13}C spectrum, the intensities of many of the carbon resonances increase significantly above those observed in a proton-coupled experiment. Carbon atoms with hydrogen atoms directly attached are enhanced the most, and the enhancement increases (but not always linearly) as more hydrogens are attached. This effect is known as the nuclear Overhauser effect, and the degree of increase in the signal is called the **nuclear Overhauser enhancement (NOE)**. The NOE effect is *heteronuclear* in this case, operating between two dissimilar atoms (carbon and hydrogen). Both atoms exhibit spins and are NMR active. The nuclear Overhauser effect is general, showing up when one of two different types of atoms is irradiated while the NMR spectrum of the other type is determined. If the absorption intensities of the observed (i.e., nonirradiated) atom change, enhancement has occurred. The effect can be either positive or negative, depending on which atom types are involved. In the case of carbon-13 interacting with hydrogen-1, the effect is positive; irradiating the hydrogens increases the intensities of the carbon signals. The maximum enhancement that can be observed is given by the relationship

$$\text{NOE}_{\text{max}} = \frac{1}{2} \left(\frac{\gamma_{\text{irr}}}{\gamma_{\text{obs}}} \right) \quad \text{Equation 4.1}$$

where γ_{irr} is the magnetogyric ratio of the nucleus being irradiated and γ_{obs} is that of the nucleus being observed. Remember that NOE_{max} is the *enhancement* of the signal, and it must be added to the original signal strength:

$$\text{total predicted intensity (maximum)} = 1 + \text{NOE}_{\text{max}} \quad \text{Equation 4.2}$$

For a proton-decoupled ^{13}C spectrum, we would calculate, using the values in Table 3.2,

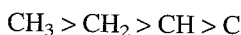
$$\text{NOE}_{\text{max}} = \frac{1}{2} \left(\frac{267.5}{67.28} \right) = 1.988 \quad \text{Equation 4.3}$$

indicating that the ^{13}C signals can be enhanced up to 200% by irradiation of the hydrogens. This value, however, is a theoretical maximum, and most actual cases exhibit less than ideal enhancement.

The heteronuclear NOE effect actually operates in both directions; either atom can be irradiated. If one were to irradiate carbon-13 while determining the NMR spectrum of the hydrogens—the reverse of the usual procedure—the hydrogen signals would increase by a very small amount. However, because there are few ^{13}C atoms in a given molecule, the result would not be very dramatic. In contrast, NOE is a definite *bonus* received in the determination of proton-decoupled ^{13}C spectra. The hydrogens are numerous, and carbon-13, with its low abundance, generally produces weak signals. Because NOE increases the intensity of the carbon signals, it substantially increases the sensitivity (signal-to-noise ratio) in the ^{13}C spectrum.

Signal enhancement due to NOE is an example of **cross-polarization**, in which a polarization of the spin states in one type of nucleus causes a polarization of the spin states in another nucleus. Cross-polarization will be explained in Section 4.6. In the current example (proton-decoupled ^{13}C spectra), when the hydrogens in the molecule are irradiated, they become saturated and attain a distribution of spins very different from their equilibrium (Boltzmann) state. There are more spins than normal in the *excited* state. Due to the interaction of spin dipoles, the spins of the carbon nuclei “sense” the spin imbalance of the hydrogen nuclei and begin to adjust themselves to a new equilibrium state that has more spins in the *lower* state. This increase of population in the lower spin state of carbon increases the intensity of the NMR signal.

In a proton-decoupled ^{13}C spectrum, the total NOE for a given carbon increases as the number of nearby hydrogens increases. Thus, we usually find that the intensities of the signals in a ^{13}C spectrum (assuming a single carbon of each type) assume the order



Although the hydrogens producing the NOE effect influence carbon atoms more distant than the ones to which they are attached, their effectiveness drops off rapidly with distance. The interaction of the spin-spin dipoles operates through space, not through bonds, and its magnitude decreases as a function of the inverse of r^3 , where r is the radial distance from the hydrogen of origin.

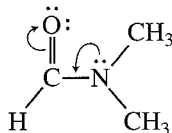
$$\text{C} \xrightarrow{r} \text{H} \quad \text{NOE} = f\left(\frac{1}{r^3}\right)$$

Thus, nuclei must be rather close together in the molecule in order to exhibit the NOE effect. The effect is greatest for hydrogens that are directly attached to carbon.

In advanced work, NOEs are sometimes used to verify peak assignments. Irradiation of a selected hydrogen or group of hydrogens leads to a greater enhancement in the signal of the closer of the two carbon atoms being considered. In dimethylformamide, for instance, the two methyl groups

are nonequivalent, showing two peaks at 31.1 and 36.2 ppm, because free rotation is restricted about the C–N bond due to resonance interaction between the lone pair on nitrogen and the π bond of the carbonyl group.

anti, 31.1 ppm



syn, 36.2 ppm

Dimethylformamide

Irradiation of the aldehyde hydrogen leads to a larger NOE for the carbon of the *syn* methyl group (36.2 ppm) than for that of the *anti* methyl group (31.1 ppm), allowing the peaks to be assigned. The *syn* methyl group is closer to the aldehyde hydrogen.

It is possible to retain the benefits of NOE even when determining a proton-coupled ^{13}C NMR spectrum that shows the attached hydrogen multiplets. The favorable perturbation of spin-state populations builds up slowly during irradiation of the hydrogens by the decoupler, and it persists for some time after the decoupler is turned off. In contrast, decoupling is available only while the decoupler is in operation and stops immediately when the decoupler is switched off. One can build up the NOE effect by irradiating with the decoupler during a period before the pulse and then turning off the decoupler during the pulse and free-induction decay (FID) collection periods. This technique gives an **NOE-enhanced proton-coupled spectrum**, with the advantage that peak intensities have been increased due to the NOE effect. See Section 10.1 for details.

4.6 CROSS-POLARIZATION: ORIGIN OF THE NUCLEAR OVERHAUSER EFFECT

To see how cross-polarization operates to give nuclear Overhauser enhancement, consider the energy diagram shown in Figure 4.6. Consider a two-spin system between atoms ^1H and ^{13}C . These two atoms may be spin coupled, but the following explanation is easier to follow if we simply ignore any spin–spin splitting. The following explanation is applied to the case of ^{13}C NMR spectroscopy, although the explanation is equally applicable to other possible combinations of atoms. Figure 4.6 shows four separate energy levels (N_1 , N_2 , N_3 , and N_4), each with a different combination of spins of atoms ^1H and ^{13}C . The spins of the atoms are shown at each energy level.

The selection rules, derived from quantum mechanics, require that the only allowed transitions involve a change of only one spin at a time (these are called **single-quantum transitions**). The allowed transitions, proton excitations (labeled ^1H) and carbon excitations (labeled ^{13}C), are shown. Notice that both proton transitions and both carbon transitions have the same energy (remember that we are ignoring splitting due to J interactions).

Because the four spin states have different energies, they also have different *populations*. Because the spin states N_3 and N_2 have very similar energies, we can assume that their populations are approximately equal. Now use the symbol B to represent the equilibrium populations of these two spin states. The population of spin state N_1 , however, will be higher (by an amount δ), and the population of spin state N_4 will be reduced (also by an amount δ). The intensities of the NMR lines will be proportional to the difference in populations between the energy levels where transitions are occurring. If we compare the populations of each energy level, we can see that the intensities of the two carbon lines (X) will be equal.

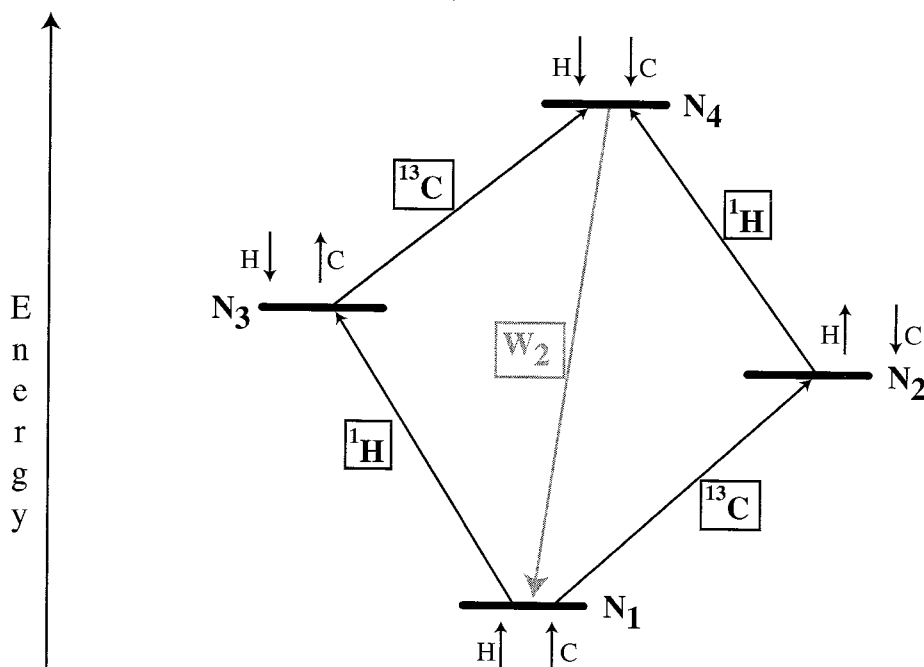


FIGURE 4.6 Spin energy level diagram for an AX System.

Level	Equilibrium Populations
N_1	$B + \delta$
N_2	B
N_3	B
N_4	$B - \delta$

Assuming that the populations of the ^{13}C energy levels are at equilibrium, the carbon signals will have intensities:

^{13}C Energy Levels at Equilibrium

$$N_3 - N_4 = B - B + \delta = \delta$$

$$N_1 - N_2 = B + \delta - B = \delta$$

Consider now what happens when we irradiate the proton transitions during the broad-band decoupling procedure. The irradiation of the protons causes the proton transitions to become **saturated**. In other words, the probability of an upward and a downward transition for these nuclei (the proton transitions shown in Fig. 4.6) now becomes *equal*. The population of level N_4 becomes equal to the population of level N_2 , and the population of level N_3 is now equal to the population of level N_1 . The populations of the spin states can now be represented by the following expressions.

PROTON DECOUPLED	
Level	Populations
N_1	$B + \frac{1}{2}\delta$
N_2	$B - \frac{1}{2}\delta$
N_3	$B + \frac{1}{2}\delta$
N_4	$B - \frac{1}{2}\delta$

Using these expressions, the intensities of the carbon lines can be represented:

^{13}C Energy Levels with Broad-Band Decoupling

$$N_3 - N_4 = B + \frac{1}{2}\delta - B - \frac{1}{2}\delta = \delta$$

$$N_1 - N_2 = B + \frac{1}{2}\delta - B + \frac{1}{2}\delta = \delta$$

So far, there has been no change in the intensity of the carbon transition.

At this point we need to consider that there is another process operating in this system. When the populations of the spin states have been disturbed from their equilibrium values, as in this case by irradiation of the proton signal, **relaxation processes** will tend to restore the populations to their equilibrium values. Unlike excitation of a spin from a lower to a higher spin state, relaxation process are not subject to the same quantum mechanical selection rules. Relaxation involving changes of both spins simultaneously (called **double-quantum transitions**) are allowed; in fact they are relatively important in magnitude. The relaxation pathway labeled W_2 in Fig. 4.6 tends to restore equilibrium populations by relaxing spins from state N_4 to N_1 . We shall represent the number of spins that are relaxed by this pathway by the symbol d . The populations of the spin states thus become as follows:

Level	Populations
N_1	$B + \frac{1}{2}\delta + d$
N_2	$B - \frac{1}{2}\delta$
N_3	$B + \frac{1}{2}\delta$
N_4	$B - \frac{1}{2}\delta - d$

The intensities of the carbon lines can now be represented:

^{13}C Energy Levels with Broad-Band Decoupling and with Relaxation

$$N_3 - N_4 = B + \frac{1}{2}\delta - B + \frac{1}{2}\delta + d = \delta + d$$

$$N_1 - N_2 = B + \frac{1}{2}\delta + d - B + \frac{1}{2}\delta = \delta + d$$

Thus the intensity of each of the carbon lines has been enhanced by an amount d because of this relaxation.

The theoretical maximum value of d is 2.988 (see Equations 4.2 and 4.3). The amount of nuclear Overhauser enhancement that may be observed, however, is often less than this amount. The pre-

ceding discussion has ignored possible relaxation from state N_3 to N_2 . This relaxation pathway would involve no net change in the total number of spins (a **zero-quantum transition**). This relaxation would tend to *decrease* the nuclear Overhauser enhancement. With relatively small molecules, this second relaxation pathway is much less important than W_2 ; therefore, we generally see a substantial enhancement.

4.7 PROBLEMS WITH INTEGRATION IN ^{13}C Spectra

Avoid attaching too much significance to peak sizes and integrals in proton-decoupled ^{13}C spectra. In fact, carbon spectra are usually not integrated in the same routine fashion as is accepted for proton spectra. Integral information derived from ^{13}C spectra is usually not reliable unless special techniques are used to ensure its validity. It is true that a peak derived from two carbons is larger than one derived from a single carbon. However, as we saw in Section 4.5, if decoupling is used, the intensity of a carbon peak is NOE enhanced by any hydrogens that are either attached to that carbon or found close by. Nuclear Overhauser enhancement is not the same for every carbon. Recall that as a very rough approximation (with some exceptions), a CH_3 peak generally has a greater intensity than a CH_2 peak, which in turn has a greater intensity than a CH peak, and quaternary carbons, those without any attached hydrogens, are normally the weakest peaks in the spectrum.

A second problem arises in the measurement of integrals in ^{13}C FT-NMR. Figure 4.7 shows the typical pulse sequence for an FT-NMR experiment. Repetitive pulse sequences are spaced at intervals of about 1 to 3 seconds. Following the pulse, the time allotted to collect the data (the FID) is called the **acquisition time**. A short **delay** usually follows the acquisition of data. When hydrogen spectra are determined, it is common for the FID to have decayed to zero before the end of the acquisition time. Most hydrogen atoms relax back to their original Boltzmann condition very quickly—within less than a second. For ^{13}C atoms, however, the time required for relaxation is quite variable, depending on the molecular environment of the particular atom (see Section 4.8). Some ^{13}C atoms relax very quickly (in seconds), but others require quite long periods (minutes) compared to hydrogen. If carbon atoms with long relaxation times are present in a molecule, collection of the FID signal may have already ceased before all of the ^{13}C atoms have relaxed. The result of this discrepancy is that some atoms have strong signals, as their contribution to the FID is complete, while others, those that have not relaxed completely, have weaker signals. When this happens, the resulting peak areas do not integrate to give the correct numbers of carbons.

It is possible to extend the data collection period (and the delay period) to allow all of the carbons in a molecule to relax; however, this is usually done only in special cases. Since repetitive scans are used in ^{13}C spectra, the increased acquisition time means that it would simply take too long to measure a complete spectrum with a reasonable signal-to-noise ratio.

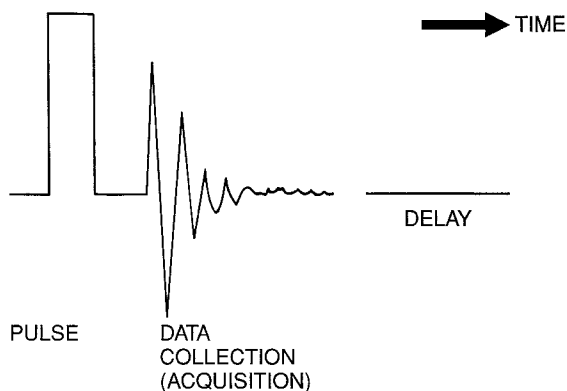


FIGURE 4.7 A typical FT-NMR pulse sequence.

4.8 MOLECULAR RELAXATION PROCESSES

In the absence of an applied field, there is a nearly 50/50 distribution of the two spin states for a nucleus of spin $=\frac{1}{2}$. A short time after a magnetic field is applied, a slight excess of nuclei builds up in the lower-energy (aligned) spin state due to thermal equilibration. We call the relative numbers of nuclei in the upper and lower states the **Boltzmann equilibrium**. In Section 3.5 we used the Boltzmann equations to calculate the expected number of excess nuclei for NMR spectrometers that operate at various frequencies (Table 3.3). We rely on these excess nuclei to generate NMR signals. When we pulse the system at the resonance frequency, we disturb the Boltzmann equilibrium (alter the spin population ratios). Excess nuclei are excited to the upper spin state and, as they **relax**, or return to the lower spin state and equilibrium, they generate the FID signal, which is processed to give the spectrum.

If all of the excess nuclei absorb energy, **saturation**, a condition in which the populations of both spin states are once again equal, is reached and the population of the upper spin state cannot be increased further. This limitation exists because further irradiation induces just as many downward transitions as there are upward transitions when the populations of both states are equal. Net signals are observed only when the populations are unequal. If irradiation is stopped, either at or before saturation, the excited excess nuclei relax and the Boltzmann equilibrium is reestablished.

The methods by which excited nuclei return to their ground state and by which the Boltzmann equilibrium is reestablished are called **relaxation processes**. In NMR systems there are two principal types of relaxation processes: spin–lattice relaxation and spin–spin relaxation. Each occurs as a first-order rate process and is characterized by a **relaxation time**, which governs the rate of decay.

Spin–lattice, or *longitudinal*, **relaxation processes** are those that occur in the direction of the field. The spins lose their energy by transferring it to the surroundings—the *lattice*—as thermal energy. Ultimately the lost energy heats the surroundings. The **spin–lattice relaxation time**, T_1 , governs the rate of this process. The inverse of the spin–lattice relaxation time, $1/T_1$, is the rate constant for the decay process.

Several processes, both within the molecule (intramolecular) and between molecules (intermolecular), contribute to spin–lattice relaxation. The principal contributor is dipole–dipole interaction. The spin of an excited nucleus interacts with the spins of other magnetic nuclei that are in the same molecule or in nearby molecules. These interactions can induce nuclear spin transitions and exchanges. Eventually the system relaxes back to the Boltzmann equilibrium. This mechanism is especially effective if there are hydrogen atoms nearby. For carbon nuclei, relaxation is fastest if hydrogen atoms are directly bonded, as in CH, CH₂, and CH₃ groups. Spin–lattice relaxation is also most effective in larger molecules, which tumble (rotate) slowly, and it is very inefficient in small molecules, which tumble faster.

Spin–spin, or *transverse*, **relaxation processes** are those that occur in a plane perpendicular to the direction of the field—the same plane in which the signal is detected. Spin–spin relaxation does not change the energy of the spin system. It is often described as an entropy process. When nuclei are induced to change their spin by the absorption of radiation, they all end up precessing in phase after resonance. This is called **phase coherence**. The nuclei lose the phase coherence by exchanging spins. The phases of the precessing spins randomize (increase entropy). This process occurs only between nuclei of the same type—those that are studied in the NMR experiment. The **spin–spin relaxation time**, T_2 , governs the rate of this process.

Our interest is in spin–lattice relaxation times, T_1 (rather than spin–spin relaxation times), as they relate to the intensity of NMR signals and have other implications relevant to structure determination. T_1 relaxation times are relatively easy to measure by the **inversion recovery method**.² Spin–spin relaxation times, T_2 , are more difficult to measure and do not provide useful structural in-

²Consult the references listed at the end of the chapter for the details of this method.

formation. Spin-spin relaxation (phase randomization) always occurs more quickly than the rate at which spin-lattice relaxation returns the system to Boltzmann equilibrium ($T_2 \leq T_1$). However, for nuclei with spin = $\frac{1}{2}$ and a solvent of low viscosity, T_1 and T_2 are usually very similar.

Spin-lattice relaxation times, T_1 values, are not of much use in proton NMR since protons have very short relaxation times. However, T_1 values are quite important to ^{13}C NMR spectra because they are much longer for carbon nuclei and can dramatically influence signal intensities. One can always expect quaternary carbons (including most carbonyl carbons) to have long relaxation times because they have no attached hydrogens. A common instance of long relaxation times is the carbons in an aromatic ring with a substituent group different from hydrogen. The ^{13}C T_1 values for isooctane (2,2,4-trimethylpentane) and toluene follow.

	C	T_1
	1, 6, 7	9.3 sec
	2	68
	3	13
	4	23
	5, 8	9.8

2,2,4-Trimethylpentane

	C	T_1	NOE
	α	16 sec	0.61
	1	89	0.56
	2	24	1.6
	3	24	1.7
	4	17	1.6

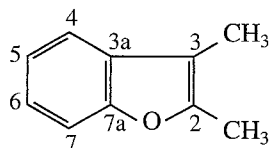
Toluene

Notice that in isooctane the quaternary carbon 2, which has no attached hydrogens, has the longest relaxation time (68 sec). Carbon 4, which has one hydrogen, has the next longest (23 sec) and is followed by carbon 3, which has two hydrogens (13 sec). The methyl groups (carbons 1, 5, 6, 7, and 8) have the shortest relaxation times in this molecule. The NOE factors for toluene have been listed along with the T_1 values. As expected, the *ipso* carbon 1, which has no hydrogens, has the longest relaxation time and the smallest NOE. In the ^{13}C NMR of toluene, the *ipso* carbon has the lowest intensity.

Remember also that T_1 values are greater when a molecule is small and tumbles rapidly in the solvent. The carbons in cyclopropane have a T_1 of 37 sec. Cyclohexane has a smaller value, 20 sec. In a larger molecule such as the steroid cholesterol, all of the carbons except those that are quaternary would be expected to have T_1 values less than 1 to 2 sec. The quaternary carbons would have T_1 values of about 4 to 6 sec due to the lack of attached hydrogens. In solid polymers, such as polystyrene, the T_1 values for the various carbons are around 10^{-2} sec.

To interpret ^{13}C NMR spectra, you should know what effects of NOE and spin-lattice relaxation to expect. We cannot fully cover the subject here, and there are many additional factors besides those that we have discussed. If you are interested, consult more advanced textbooks, such as the ones listed in the references.

The example of 2,3-dimethylbenzofuran will close this section. In this molecule, the quaternary (*ipso*) carbons have relaxation times that exceed 1 minute. As discussed in Section 4.7, to obtain a decent spectrum of this compound, it would be necessary to extend the data acquisition and delay periods so as to determine the entire spectrum of the molecule and see the carbons with high T_1 values.



C	T_1	NOE
2	83 sec	1.4
3	92	1.6
3a	114	1.5
7a	117	1.3
Others	<10	1.6–2

2,3-Dimethylbenzofuran

4.9 OFF-RESONANCE DECOUPLING

The decoupling technique that is used to obtain typical proton-decoupled spectra has the advantage that all peaks become singlets. For carbon atoms bearing attached hydrogens, an added benefit is that peak intensities increase, owing to the nuclear Overhauser effect, and signal-to-noise ratios improve. Unfortunately, much useful information is also lost when carbon spectra are decoupled. We no longer have information about the number of hydrogens that are attached to a particular carbon atom.

In many cases it would be helpful to have the information about the attached hydrogens that a proton-coupled spectrum provides, but frequently the spectrum becomes too complex, with overlapping multiplets that are difficult to resolve or assign correctly. A compromise technique called **off-resonance decoupling** can often provide multiplet information while keeping the spectrum relatively simple in appearance.

In an off-resonance-decoupled ^{13}C spectrum, the coupling between each carbon atom and each hydrogen attached directly to it is observed. The $n + 1$ Rule can be used to determine whether a given carbon atom has three, two, one, or no hydrogens attached. However, when off-resonance decoupling is used, the *apparent magnitude* of the coupling constants is reduced, and overlap of the resulting multiplets is a less frequent problem. The off-resonance-decoupled spectrum retains the couplings between the carbon atom and directly attached protons (the one-bond couplings) but effectively removes the couplings between the carbon and more remote protons.

In this technique, the frequency of a second radiofrequency transmitter (the **decoupler**) is set either upfield or downfield from the usual sweep width of a normal proton spectrum (i.e., *off resonance*). In contrast, the frequency of the decoupler is set to *coincide exactly* with the range of proton resonances in a true decoupling experiment. Furthermore, in off-resonance decoupling, the power of the decoupling oscillator is held *low* to avoid complete decoupling.

Off-resonance decoupling can be a great help in assigning spectral peaks. The off-resonance-decoupled spectrum is usually obtained separately, along with the proton-decoupled spectrum. Figure 4.8 shows the off-resonance-decoupled spectrum of 1-propanol, in which the methyl carbon atom is split into a quartet and each of the methylene carbons appears as a triplet. Notice that the observed multiplet patterns are consistent with the $n + 1$ Rule and with the patterns shown in Figure 4.3. If TMS had been added, its methyl carbons would have appeared as a quartet centered at $\delta = 0$ ppm.

4.10 A QUICK DIP INTO DEPT

Despite its utility, off-resonance decoupling is now considered an old-fashioned technique. It has been replaced by more modern methods, the most important of which is **Distortionless Enhancement by Polarization Transfer**, better known as **DEPT**. The DEPT technique requires an FT-pulsed spectrometer. It is more complicated than off-resonance decoupling and it requires a computer, but it gives the same information more reliably and more clearly. Chapter 10 will discuss the DEPT

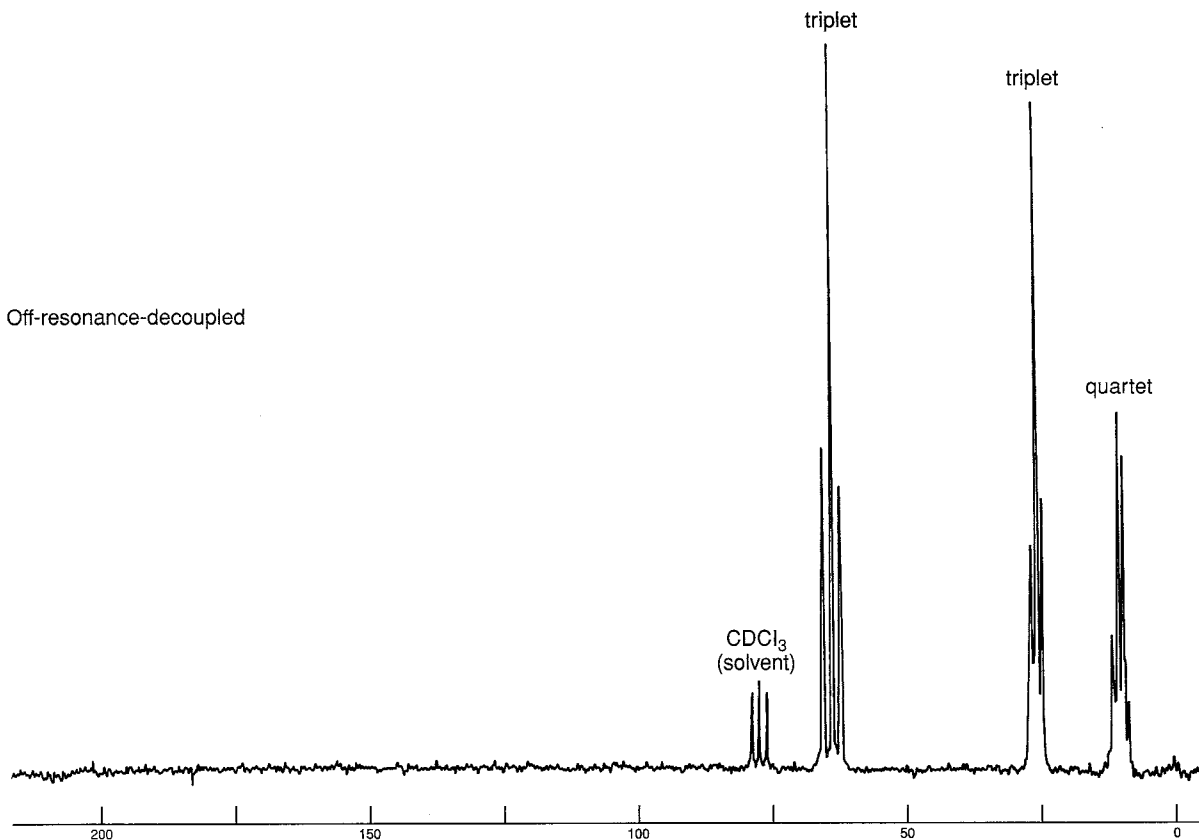
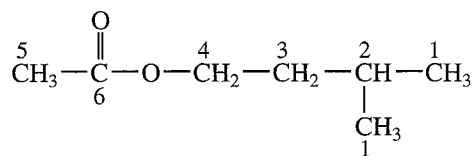


FIGURE 4.8 The off-resonance-decoupled ^{13}C spectrum of 1-propanol (22.5 MHz).

method in detail; only a brief introduction to the method and the results it provides will be provided here.

In the DEPT technique, the sample is irradiated with a complex sequence of pulses in both the ^{13}C and ^1H channels. The result of these pulse sequences³ is that the ^{13}C signals for the carbon atoms in the molecule will exhibit different **phases**, depending on the number of hydrogens attached to each carbon. Each type of carbon will behave slightly differently, depending on the **duration** of the complex pulses. These differences can be detected, and spectra produced in each experiment can be plotted.

One common method of presenting the results of a DEPT experiment is to plot four different **subspectra**. Each subspectrum provides different information. A sample DEPT plot for **isopentyl acetate** is shown in Figure 4.9.



³Pulse sequences were introduced in Section 4.7.

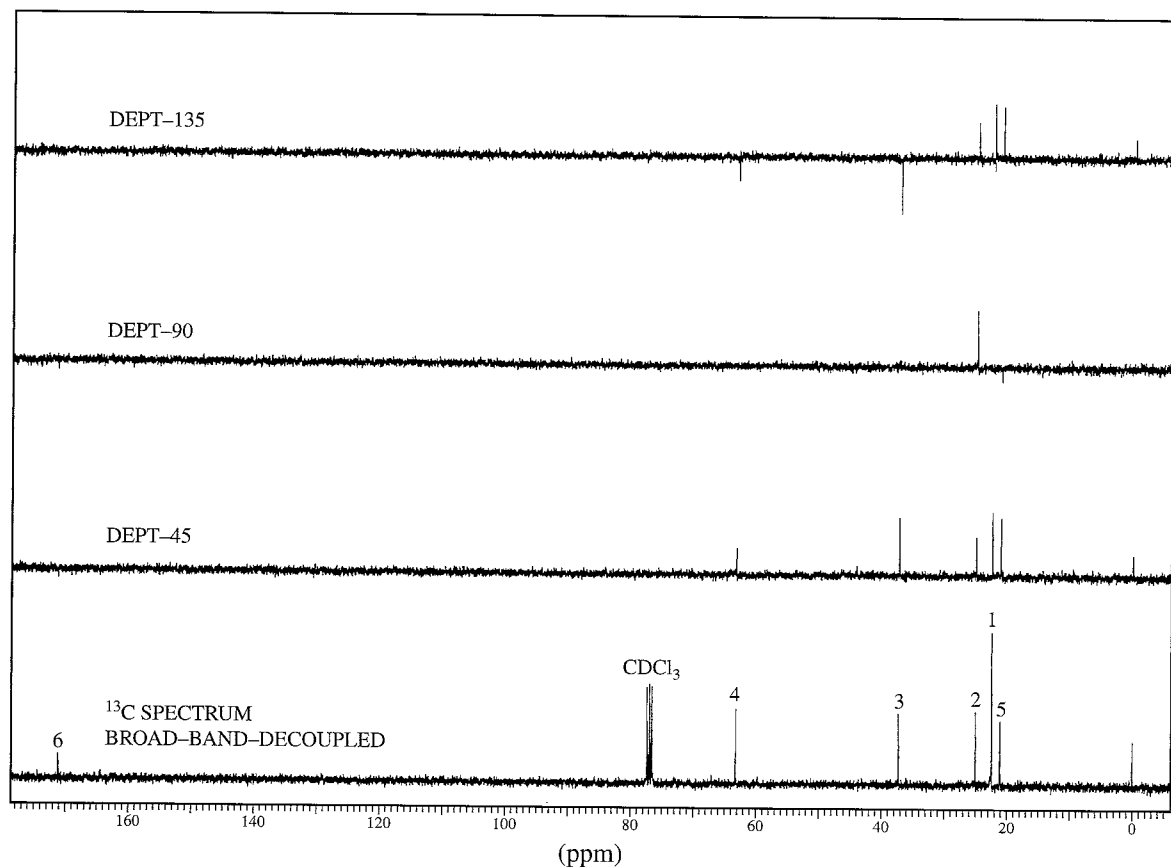


FIGURE 4.9 DEPT spectra of isopentyl acetate.

The lowest trace in the figure is the usual broad-band-decoupled ^{13}C spectrum. The second trace from the bottom is the result of a pulse sequence (called a **DEPT-45**) in which the only signals detected are those that arise from protonated carbons. You will notice that the carbonyl carbon (labeled **6**), at 172 ppm, is not seen. The solvent peaks arising from CDCl_3 (77 ppm) are also not seen. Deuterium (D or ^2H) behaves differently from ^1H , and as a result the carbon of CDCl_3 behaves as if it were not protonated. The third trace is the result of a slightly different pulse sequence (called a **DEPT-90**). In this trace, only those carbons that bear a single hydrogen are seen. Only the carbon at position **2** (25 ppm) is observed.

The uppermost trace is more complicated than the previous subspectra. The pulse sequence that gives rise to this subspectrum is called **DEPT-135**. Here all carbons that have an attached proton provide a signal, but the **phase** of the signal will be different, depending on whether the number of attached hydrogens is an odd or an even number. Signals arising from CH or CH_3 groups will give positive peaks, while signals arising from CH_2 groups will form negative (inverse) peaks. When we examine the upper trace in Figure 4.9, we can identify all of the carbon peaks in the spectrum of isopentyl acetate. The positive peaks at 21 and 22 ppm must represent CH_3 groups, as those peaks are not represented in the DEPT-90 subspectrum. When we look at the original ^{13}C spectrum, we see that the peak at 21 ppm is not as strong as the peak at 22 ppm. We conclude, therefore, that the peak at 21 ppm must come from the CH_3 carbon at position **5**, while the stronger peak at 22 ppm comes from the pair of equivalent CH_3 carbons at position **1**. We have already determined that the positive peak at 25 ppm is due to the CH carbon at position **2**, as it appears in both the DEPT-135 and the DEPT-90 subspectra. The inverse peak at 37 ppm is due to a CH_2 group, and we can identify it as coming from the carbon at position **3**. The inverse peak at 53 ppm is clearly caused by the CH_2

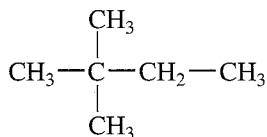
carbon at position 4, deshielded by the attached oxygen atom. Finally, the downfield peak at 172 ppm has already been labeled as arising from the carbonyl carbon at 6. This peak appears only in the original ^{13}C spectrum; therefore, it must not have any attached hydrogens.

Through the mathematical manipulation of the results of each of the different DEPT pulse sequences, it is also possible to present the results as a series of subspectra in which only the CH carbons appear in one trace, only the CH_2 carbons appear in the second trace, and only the CH_3 carbons appear in the third trace. Another common means of displaying DEPT results is to show only the result of the DEPT-135 experiment. The spectroscopist generally can interpret the results of this spectrum by applying knowledge of likely chemical shift differences to distinguish between CH and CH_3 carbons.

The results of DEPT experiments may be used from time to time in this textbook to help you solve assigned exercises. In an effort to save space, most often only the results of the DEPT experiment, rather than the complete spectrum, will be provided.

4.11 SOME SAMPLE SPECTRA—EQUIVALENT CARBONS

Equivalent ^{13}C atoms appear at the same chemical shift value. Figure 4.10 shows the proton-decoupled carbon spectrum for 2,2-dimethylbutane. The three methyl groups at the left side of the molecule are equivalent by symmetry.



Although this compound has a total of six carbons, there are only four peaks in the ^{13}C NMR spectrum. The ^{13}C atoms that are equivalent appear at the same chemical shift. The single methyl carbon, **a**, appears at highest field (9 ppm), while the three equivalent methyl carbons, **b**, appear at 29 ppm. The quaternary carbon **c** gives rise to the small peak at 30 ppm, and the methylene carbon **d** appears at 37 ppm. The relative sizes of the peaks are related, in part, to the number of each type of carbon atom present in the molecule. For example, notice in Figure 4.10 that the peak at 29 ppm (**b**) is much larger than the others. This peak is generated by three carbons. The quaternary carbon at 30

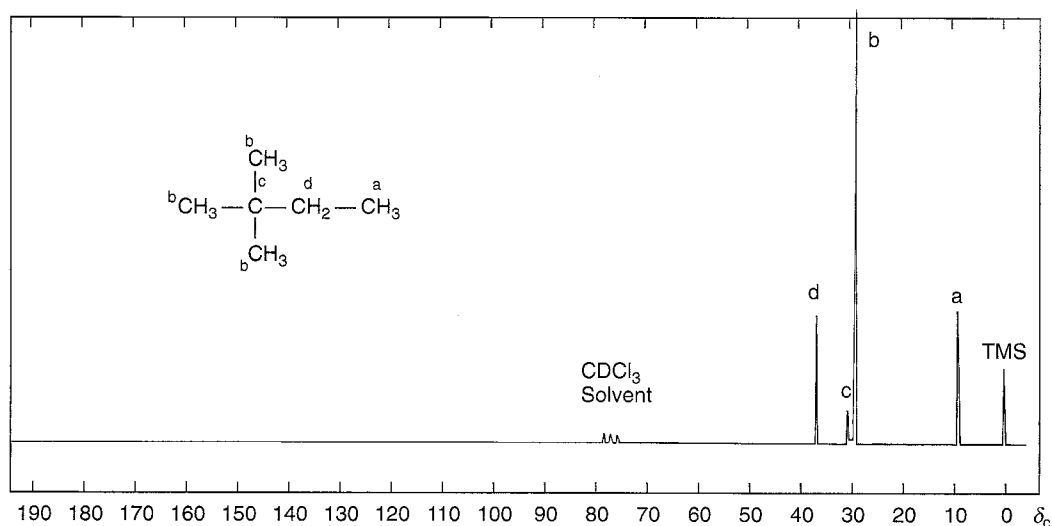


FIGURE 4.10 The proton-decoupled ^{13}C NMR spectrum of 2,2-dimethylbutane.

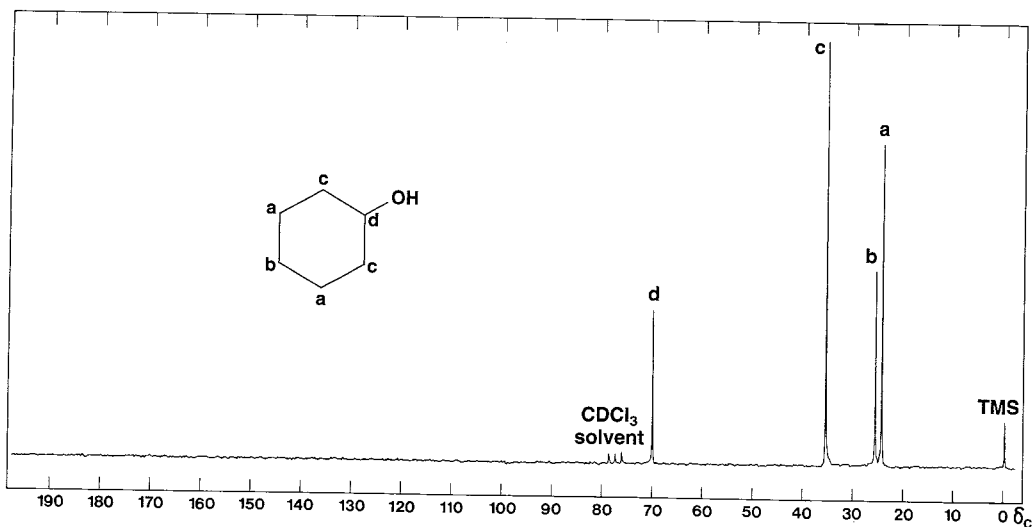


FIGURE 4.11 The proton-decoupled ^{13}C NMR spectrum of cyclohexanol.

ppm (c) is very weak. Since no hydrogens are attached to this carbon, there is very little NOE enhancement. Without attached hydrogen atoms, relaxation times are also longer than for other carbon atoms. Quaternary carbons, those with no hydrogens attached, frequently appear as weak peaks in proton-decoupled ^{13}C NMR spectra (see Sections 4.5 and 4.7).

Figure 4.11 is a proton-decoupled ^{13}C spectrum of cyclohexanol. This compound has a plane of symmetry passing through its hydroxyl group, and it shows only four carbon resonances. Carbons **a** and **c** are doubled due to symmetry and give rise to larger peaks than carbons **b** and **d**. Carbon **d**, bearing the hydroxyl group, is deshielded by oxygen and has its peak at 70.0 ppm. Notice that this peak has the lowest intensity of all of the peaks. Its intensity is lower than that of carbon **b** in part because the carbon **d** peak receives the least amount of NOE; there is only one hydrogen attached to the hydroxyl carbon, whereas each of the other carbons has two hydrogens.

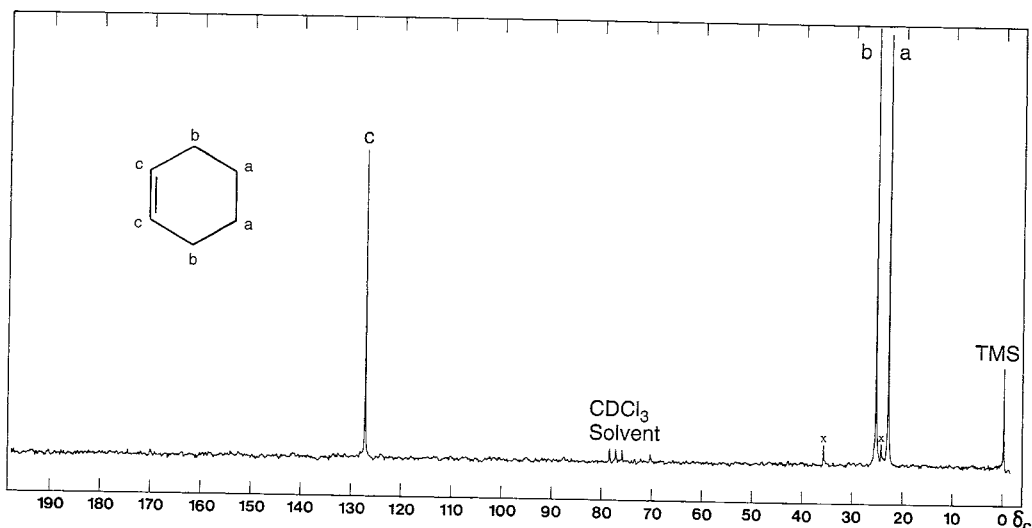


FIGURE 4.12 The proton-decoupled ^{13}C NMR spectrum of cyclohexene.

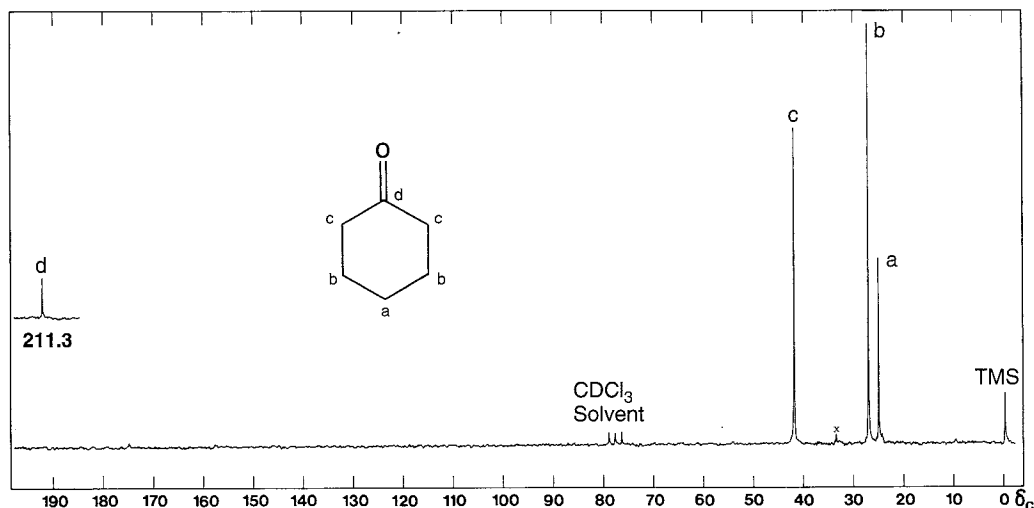


FIGURE 4.13 The proton-decoupled ^{13}C spectrum of cyclohexanone.

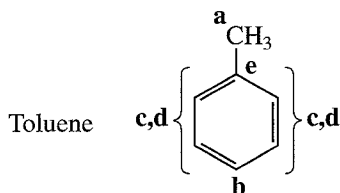
A carbon attached to a double bond is deshielded due to its sp^2 hybridization and some diamagnetic anisotropy. This effect can be seen in the ^{13}C NMR spectrum of cyclohexene (Fig. 4.12). Cyclohexene has a plane of symmetry that runs perpendicular to the double bond. As a result, we observe only three absorption peaks. There are two of each type of carbon. Each of the double-bond carbons **c** has only one hydrogen, whereas each of the remaining carbons has two. As a result of a reduced NOE, the double-bond carbons have a lower-intensity peak in the spectrum.

In Figure 4.13, the spectrum of cyclohexanone, the carbonyl carbon has the lowest intensity. This is due not only to reduced NOE (no hydrogen attached) but also to the long relaxation time of the carbonyl carbon. As you have already seen, quaternary carbons tend to have long relaxation times. Notice also that Figure 4.1 predicts the large chemical shift for this carbonyl carbon.

4.12 COMPOUNDS WITH AROMATIC RINGS

Compounds with carbon-carbon double bonds or aromatic rings give rise to chemical shifts in the range from 100 to 175 ppm. Since relatively few other peaks appear in this range, a great deal of useful information is available when peaks appear here.

A **monosubstituted** benzene ring shows *four* peaks in the aromatic carbon area of a proton-decoupled ^{13}C spectrum, since the *ortho* and *meta* carbons are doubled by symmetry. Often the carbon with no protons attached, the *ipso* carbon, has a very weak peak due to a long relaxation time and a weak NOE. In addition, there are two larger peaks for the doubled *ortho* and *meta* carbons and a medium-sized peak for the *para* carbon. In many cases, it is not important to be able to assign all of the peaks precisely. In the example of toluene, shown in Figure 4.14, notice that carbons **c** and **d** are not easy to assign by inspection of the spectrum. However, use of chemical shift correlation tables (see Section 4.2B and Appendix 8) would enable us to assign these signals.



Difficult to assign without using chemical shift correlation tables

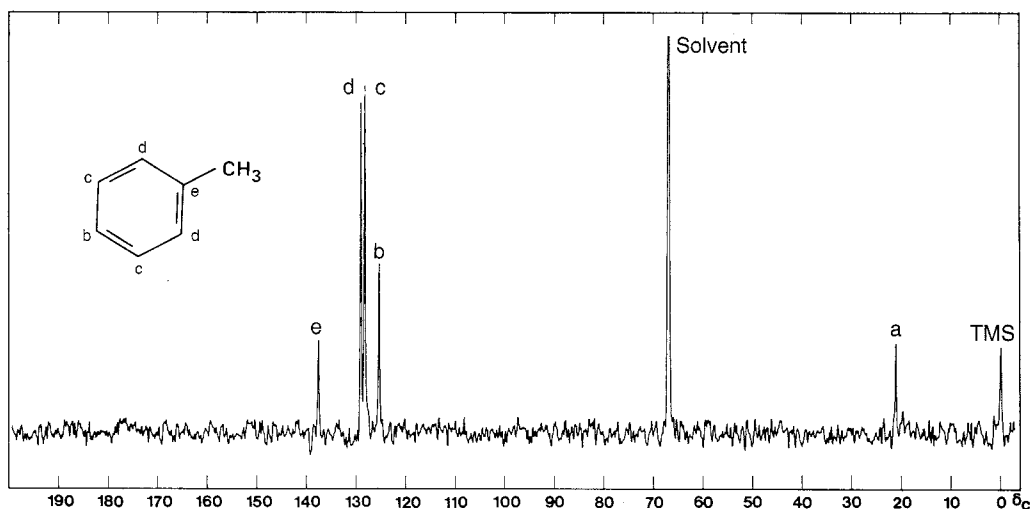
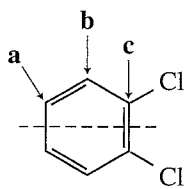


FIGURE 4.14 The proton-decoupled ^{13}C NMR spectrum of toluene.

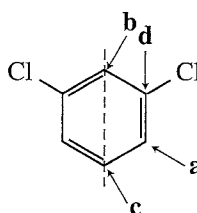
In an off-resonance-decoupled or proton-coupled ^{13}C spectrum, a monosubstituted benzene ring shows three doublets and one singlet. The singlet arises from the *ipso* carbon, which has no attached hydrogen. Each of the other carbons in the ring (*ortho*, *meta*, and *para*) has one attached hydrogen and yields a doublet.

Figure 4.4b is the proton-decoupled spectrum of ethyl phenylacetate, with the assignments noted next to the peaks. Notice that the aromatic ring region shows four peaks between 125 and 135 ppm, consistent with a monosubstituted ring. There is one peak for the methyl carbon (13 ppm) and two peaks for the methylene carbons. One of the methylene carbons is directly attached to an electronegative oxygen atom and appears at 61 ppm, while the other is more shielded (41 ppm). The carbonyl carbon (an ester) has resonance at 171 ppm. All of the carbon chemical shifts agree with the values in the correlation chart (Fig. 4.1).

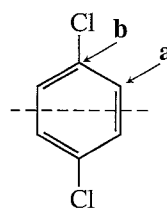
Depending on the mode of substitution, a symmetrically **disubstituted** benzene ring can show two, three, or four peaks in the proton-decoupled ^{13}C spectrum. The following drawings illustrate this for the isomers of dichlorobenzene.



Three unique carbon atoms



Four unique carbon atoms



Two unique carbon atoms

Figure 4.15 shows the spectra of all three dichlorobenzenes, each of which has the number of peaks consistent with the analysis just given. You can see that ^{13}C NMR spectroscopy is very useful in the identification of isomers.

Most other polysubstitution patterns on a benzene ring yield six different peaks in the proton-decoupled ^{13}C NMR spectrum, one for each carbon. However, when identical substituents are present, watch carefully for planes of symmetry that may reduce the number of peaks.

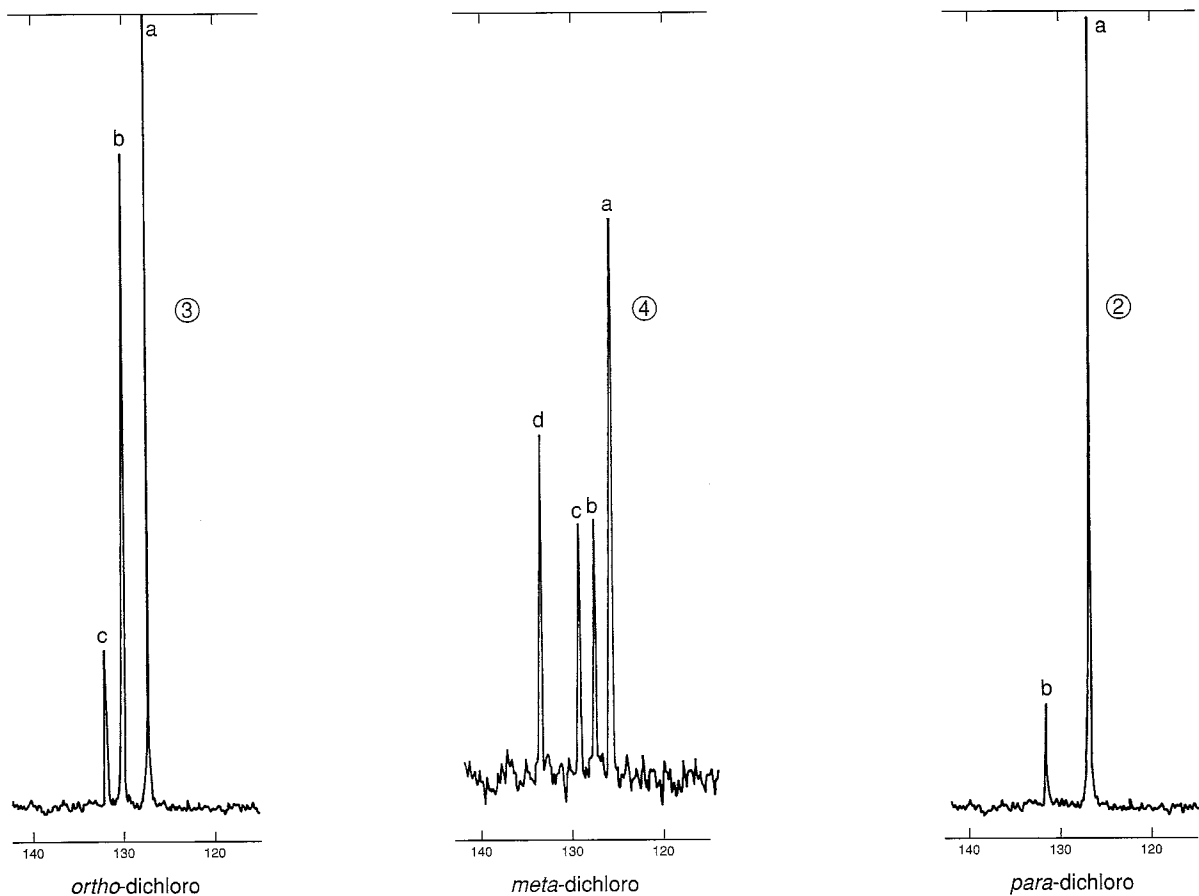


FIGURE 4.15 The proton-decoupled ^{13}C NMR spectra of the three isomers of dichlorobenzene (25 MHz).

4.13 CARBON-13 NMR SOLVENTS—HETERONUCLEAR COUPLING OF CARBON TO DEUTERIUM

Most FT-NMR spectrometers require the use of deuterated solvents because the instruments use the deuterium resonance signal as a “lock signal,” or reference signal, to keep the magnet and the electronics adjusted correctly. Deuterium is the ^2H isotope of hydrogen and can easily substitute for it in organic compounds. Deuterated solvents present few difficulties in hydrogen spectra, as the deuterium nuclei are largely invisible when a proton spectrum is determined. Deuterium has resonance at a different frequency from hydrogen. In ^{13}C NMR, however, these solvents are frequently seen as part of the spectrum, as they all have carbon atoms. In this section we explain the spectra of some of the common solvents and, in the process, examine heteronuclear coupling of carbon and deuterium. Figure 4.16 shows the ^{13}C NMR peaks due to the solvents chloroform-d and dimethylsulfoxide-d₆.

Chloroform-d, CDCl_3 , is the compound most commonly used as a solvent for ^{13}C NMR. It is also called deuteriochloroform or deuterated chloroform. Its use gives rise to a three-peak multiplet in the spectrum, with the center peak having a chemical shift of about 77 ppm. Figure 4.16 shows an example. Notice that this “triplet” is different from the triplets in a hydrogen spectrum (from two neighbors) or in a proton-coupled ^{13}C spectrum (from two attached hydrogens); the intensities are different. In this triplet, all three peaks have approximately the same intensity (1:1:1), whereas the other types of triplets have intensities that follow the entries in Pascal’s triangle, with ratios of 1:2:1.

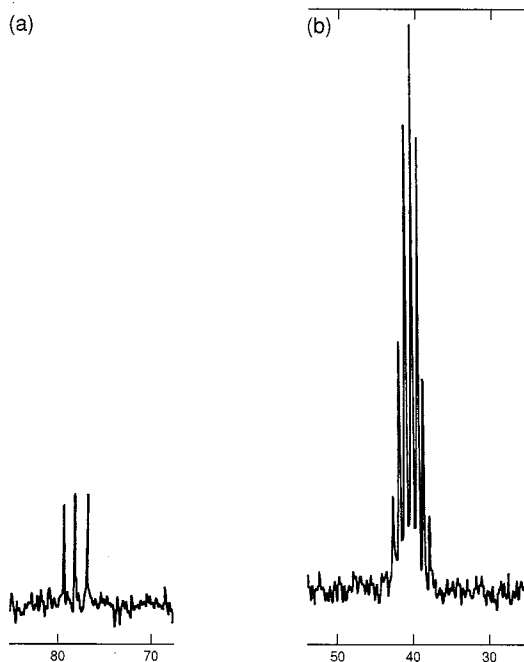


FIGURE 4.16 The ^{13}C NMR peaks of two common solvents. (a) Chloroform-d. (b) Dimethylsulfoxide-d₆.

In contrast with hydrogen (spin = $\frac{1}{2}$), deuterium has spin = 1. A single deuterium nucleus can adopt three different spins ($2I + 1 = 3$), where the spins have quantum numbers of -1 , 0 , and $+1$. In a solution of CDCl_3 , molecules can have a deuterium with any one of these spins, and as they are equally probable, we see three different chemical shifts for the carbon atom in chloroform-d. The ^{13}C -D one-bond coupling constant for this interaction is about 45 Hz. At 75 MHz these three peaks are about 0.6 ppm apart ($45 \text{ Hz}/75 \text{ MHz} = 0.60 \text{ ppm}$).

Because deuterium is not a spin = $\frac{1}{2}$ nucleus, the $n + 1$ Rule does not correctly predict the multiplicity of the carbon resonance. The $n + 1$ Rule works only for spin = $\frac{1}{2}$ nuclei and is a specialized case of a more general prediction formula:

$$\text{multiplicity} = 2nI + 1 \quad \text{Equation 4.4}$$

where n is the number of nuclei and I is the spin of that type of nucleus. If we use this formula, the correct multiplicity of the carbon peak with *one deuterium* attached is predicted by

$$2 \cdot 1 \cdot 1 + 1 = 3$$

If there are *three hydrogens*, the formula correctly predicts a quartet for the proton-coupled carbon peak:

$$2 \cdot 3 \cdot \frac{1}{2} + 1 = 4$$

Dimethylsulfoxide-d₆, $\text{CD}_3\text{-SO-CD}_3$, is frequently used as a solvent for carboxylic acids and other compounds that are difficult to dissolve in CDCl_3 . Equation 4.4 predicts a septet for the multiplicity of the carbon with three deuterium atoms attached:

$$2 \cdot 3 \cdot 1 + 1 = 7$$

This is exactly the pattern observed in Figure 4.16. The pattern has a chemical shift of 39.5 ppm, and the coupling constant is about 40 Hz.

n	$2n+1$ Lines	Relative Intensities	
0	1	1	
1	3	1	1
2	5	1	2 3 2 1
3	7	1	3 6 7 6 3 1
4	9	1	4 10 16 19 16 10 4 1
5	11	1	5 15 30 45 51 45 30 15 5 1
6	13	1	6 21 50 90 126 141 126 90 50 21 6 1

FIGURE 4.17 An intensity triangle for deuterium multiplets (n = number of deuterium atoms).

Because deuterium has $\text{spin} = 1$ instead of $\text{spin} = \frac{1}{2}$ like hydrogen, the Pascal triangle (Fig. 3.33 in Section 3.16) does not correctly predict the intensities in this seven-line pattern. Instead, a different intensity triangle must be used for splittings caused by deuterium atoms. Figure 4.17 is this intensity triangle, and Figure 4.18 is an analysis of the intensities for three-line and five-line multiplets. In the latter figure, an upward arrow represents $\text{spin} = 1$, a downward arrow represents $\text{spin} = -1$, and a large dot represents $\text{spin} = 0$. Analysis of the seven-line multiplet is left for the reader to complete.

Acetone- d_6 , $\text{CD}_3\text{-CO-CD}_3$, shows the same ^{13}C septet splitting pattern as dimethylsulfoxide- d_6 , but the multiplet is centered at 29.8 ppm with the carbonyl peak at 206 ppm. The carbonyl carbon is a singlet; three-bond coupling does not appear.

Acetone- d_5 frequently appears as an impurity in spectra determined in acetone- d_6 . It leads to interesting results in both the hydrogen and the carbon-13 spectra. Although this chapter is predominantly about carbon-13 spectra, we will examine both cases.

Hydrogen Spectrum

In proton (^1H) NMR spectra, a commonly encountered multiplet arises from a small amount of acetone- d_5 impurity in acetone- d_6 solvent. Figure 4.19 shows the multiplet, which is generated by the hydrogen in the $-\text{CHD}_2$ group of the $\text{CD}_3\text{-CO-CHD}_2$ molecule. Equation 4.4 correctly predicts that there should be a quintet in the proton spectrum of acetone- d_5 :

$$2 \cdot 2 \cdot 1 + 1 = 5$$

and this is observed.

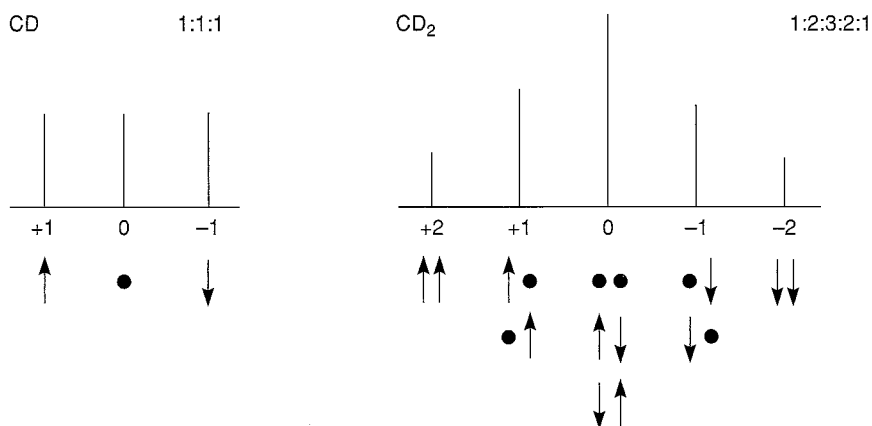


FIGURE 4.18 An intensity analysis of three- and five-line deuterium multiplets.

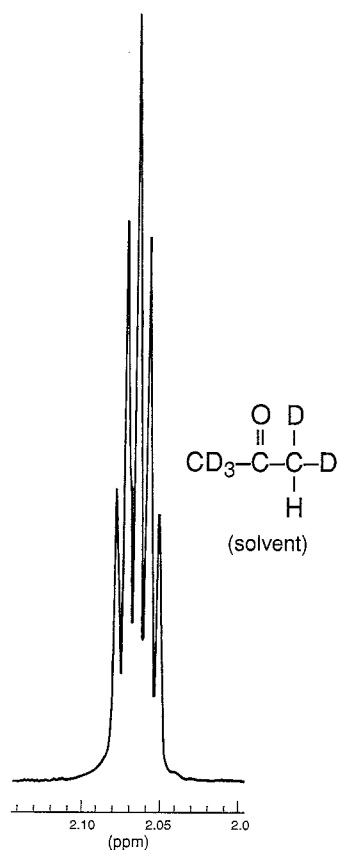


FIGURE 4.19 The 300-MHz ^1H spectrum of acetone- d_5 ($\text{CD}_3\text{-CO-CHD}_2$).

Carbon Spectrum

The proton-coupled ^{13}C spectrum of the -CHD_2 group is more complicated as both hydrogen (spin = $\frac{1}{2}$) and deuterium (spin = 1) interact with carbon. In this case we use the following formula, which is extended from Equation 4.4.

$$\text{total multiplicity} = \prod_i (2n_i I_i + 1)$$

Equation 4.5

$$\text{Condition: } I \geq \frac{1}{2}$$

The large \prod_i indicates a product of terms for each different type of atom i that couples to the atom being observed. These atoms must have spin $\geq \frac{1}{2}$; atoms of spin = 0 do not cause splitting. In the present case (-CHD_2) there are two terms, one for hydrogen and one for deuterium.

$$\text{total multiplicity} = (2 \cdot 1 \cdot \frac{1}{2} + 1)(2 \cdot 2 \cdot 1 + 1) = 10$$

The $^{13}\text{C}\text{-H}$ and $^{13}\text{C}\text{-D}$ coupling constants would most likely be different, resulting in 10 lines that would not all be equally spaced. In addition, acetone has a second “methyl” group on the other side of the carbonyl group. The -CD_3 group (seven peaks) would overlap the 10 peaks from -CHD_2 and make a pattern that would be quite difficult to decipher! The ^1H and ^{13}C chemical shifts for common NMR solvents are provided in Appendix 10.

4.14 HETERONUCLEAR COUPLING OF CARBON TO FLUORINE-19

Heteronuclear ^{13}C - ^{19}F coupling is observed when there are fluorine atoms in an organic compound. Figures 4.20 and 4.21 are two spectra that exhibit this effect.

The spectrum of CFBr_3 shows a doublet (two peaks) at 43.6 and 48.5 ppm. The ^{13}C - ^{19}F coupling constant in this example is quite large, at about 368 Hz ($4.9 \text{ ppm} \times 75 \text{ MHz} = 368 \text{ Hz}$). The second example shows both one-bond and two-bond couplings. The large quartet centered at about 124 ppm is due to the $-\text{CF}_3$ carbon. The one-bond C-F coupling constant in this case is 276 Hz (using the center two peaks of 122.49 and 126.17 ppm: $3.68 \text{ ppm} \times 75 \text{ MHz} = 276 \text{ Hz}$). The CH_2 carbon also has its resonance split by the three fluorines (two-bond coupling). This second quartet has a smaller coupling constant because the interaction operates over more bonds (using the center peaks of 61.01 and 61.47 ppm: $0.46 \text{ ppm} \times 75 \text{ MHz} = 35 \text{ Hz}$).

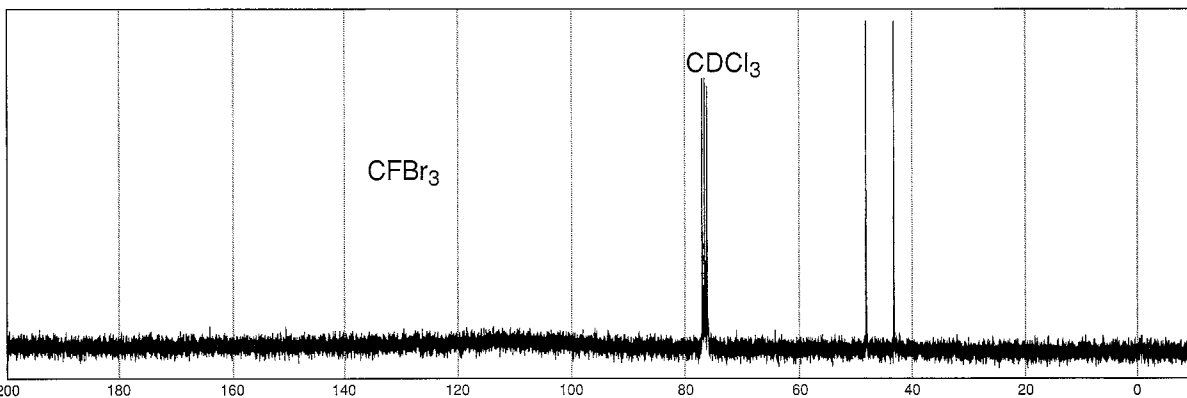


FIGURE 4.20 The ^{13}C proton-decoupled spectrum of CFBr_3 (75 MHz).

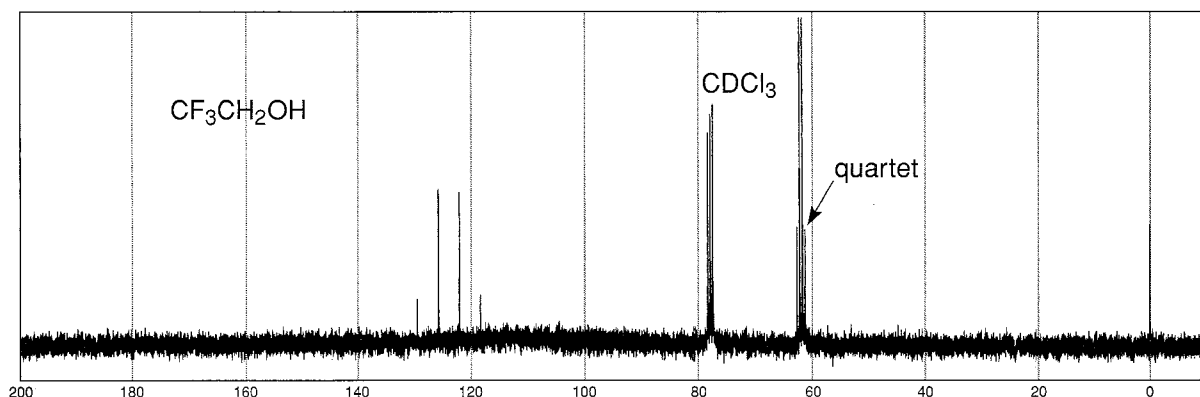


FIGURE 4.21 The ^{13}C proton-decoupled spectrum of $\text{CF}_3\text{CH}_2\text{OH}$ (75 MHz).

4.15 HETERONUCLEAR COUPLING OF CARBON TO PHOSPHORUS-31

The two spectra in Figures 4.22 and 4.23 demonstrate coupling between ^{13}C and ^{31}P . In the first compound, shown in Figure 4.22, the carbons of the methyl groups are split by phosphorus (spin = $\frac{1}{2}$) into a doublet with $J = 56$ Hz ($12.16 - 11.41 = 0.75$ ppm; 0.75 ppm \times 75 MHz = 56 Hz). This is a one-bond coupling. The second compound shows both one-bond and two-bond coupling. The one-bond coupling occurs between the phosphorus and the carbon of the methyl group, $\text{P}-\text{CH}_3$, and $J = 143$ Hz ($10.83 - 8.92 = 1.91$ ppm; 1.91 ppm \times 75 MHz = 143 Hz). The second coupling is a two-bond coupling, $\text{P}-\text{O}-\text{CH}_3$, and has a magnitude of about 7 Hz ($52.23 - 52.14 = 0.09$ ppm; 0.09 ppm \times 75 MHz = 6.75 Hz).

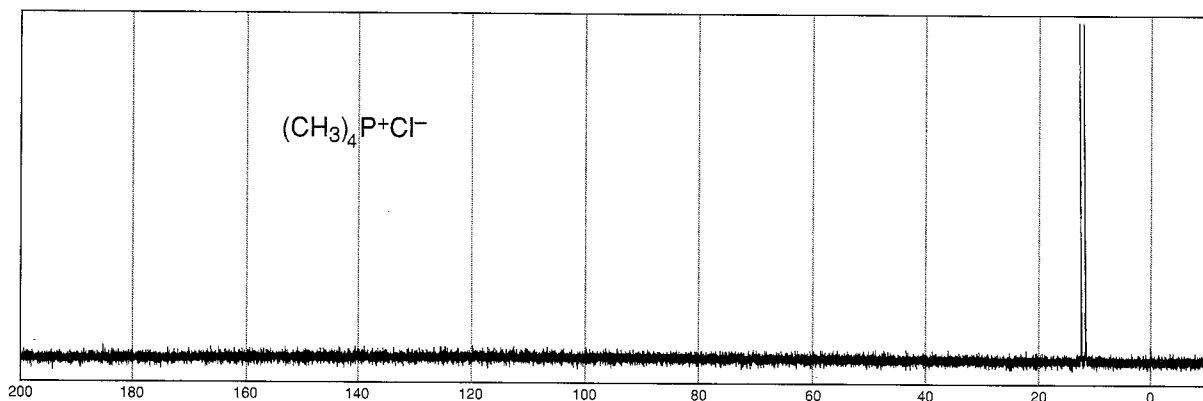


FIGURE 4.22 The ^{13}C proton-decoupled spectrum of tetramethylphosphonium chloride, $(\text{CH}_3)_4\text{P}^+\text{Cl}^-$ (75 MHz).

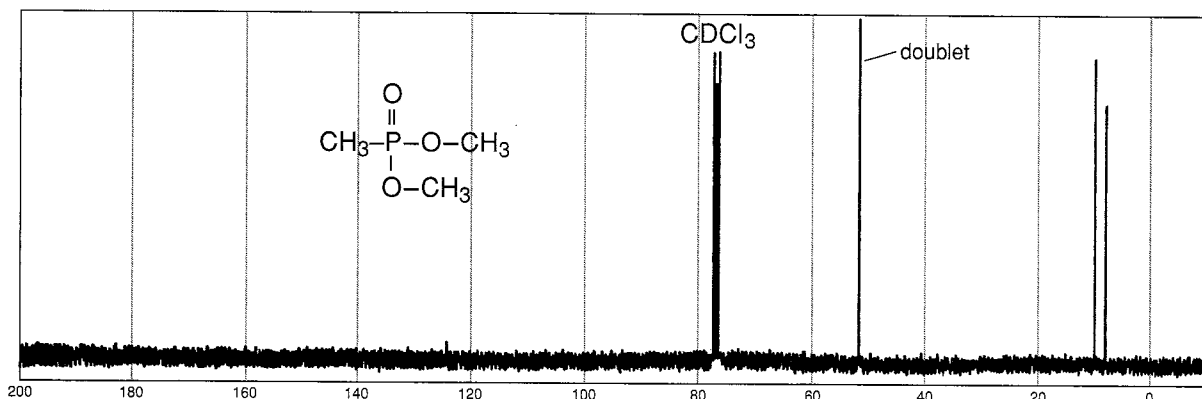
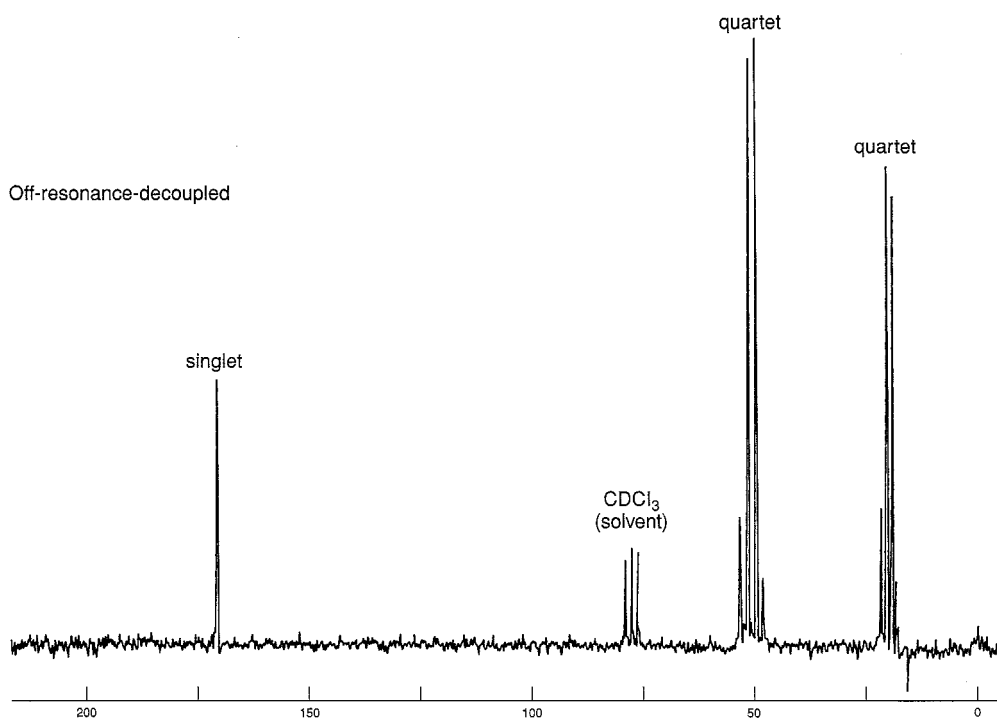
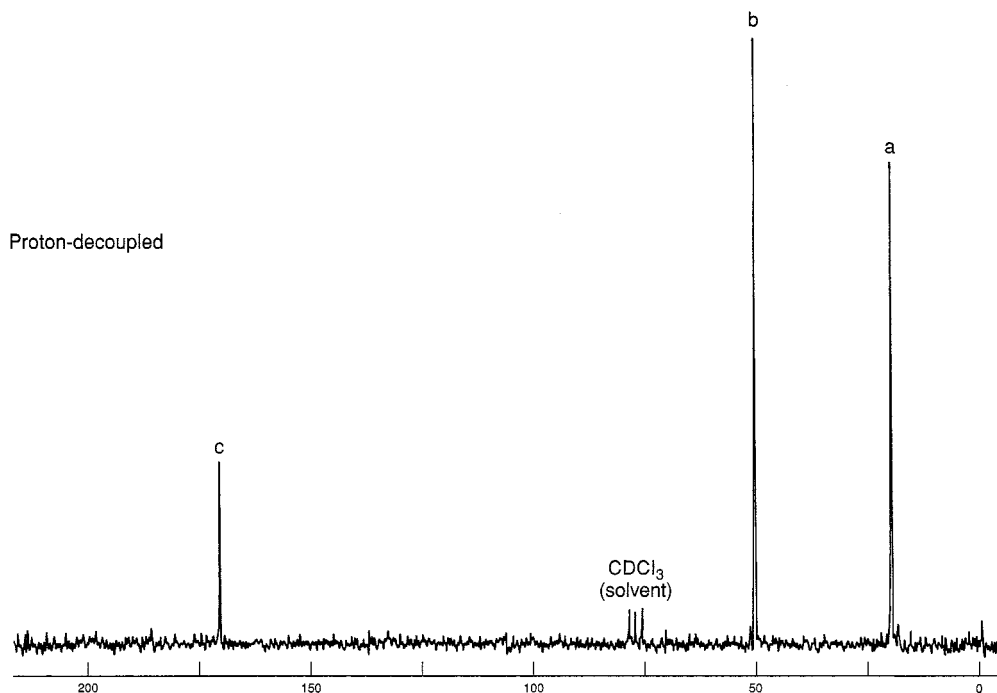


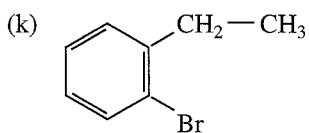
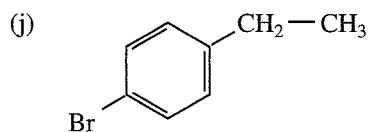
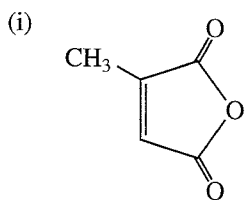
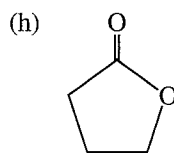
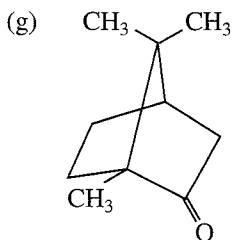
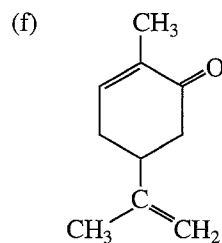
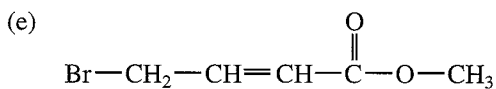
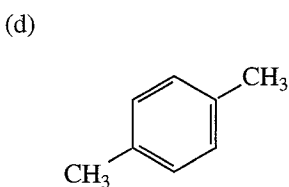
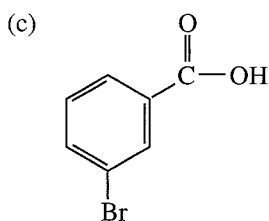
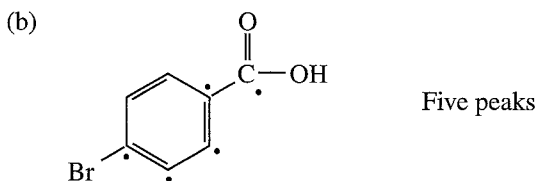
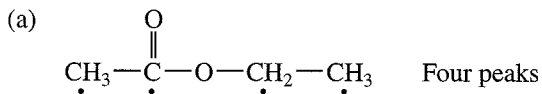
FIGURE 4.23 The ^{13}C proton-decoupled spectrum of $\text{CH}_3\text{PO}(\text{OCH}_3)_2$ (75 MHz).

PROBLEMS

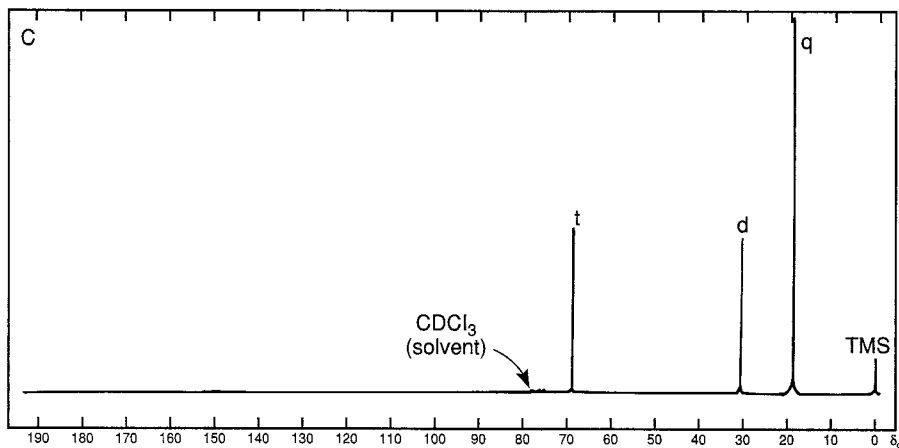
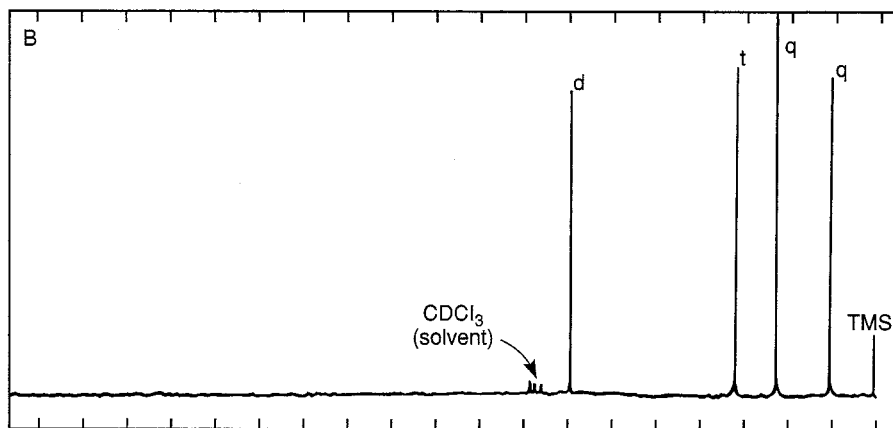
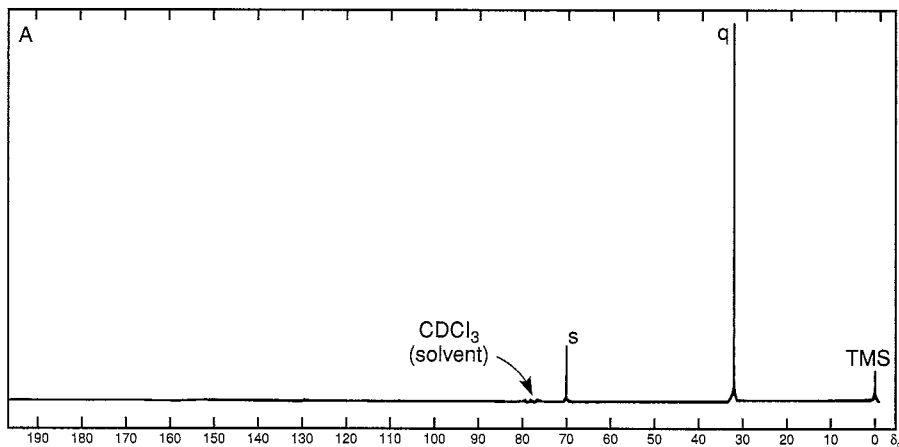
- *1. A compound with the formula $C_3H_6O_2$ gives the following proton-decoupled and off-resonance-decoupled spectra. Determine the structure of the compound.



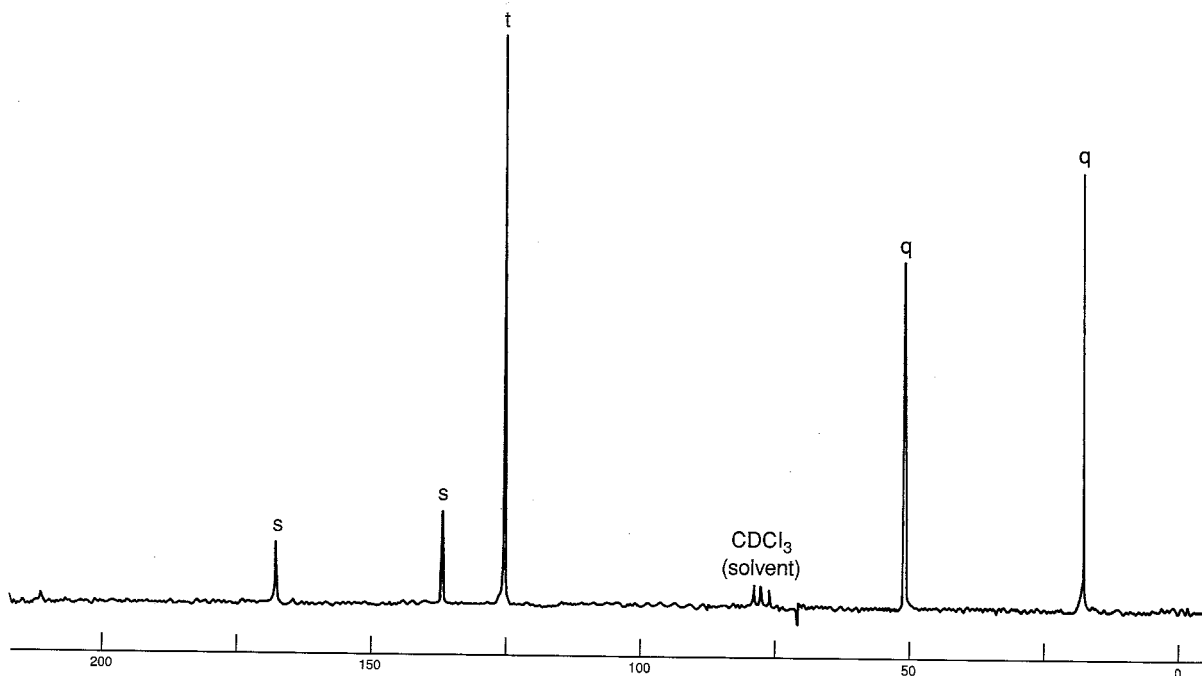
*2. Predict the number of peaks that you would expect in the proton-decoupled ^{13}C spectrum of each of the following compounds. Problems 2a and 2b are provided as examples. Dots are used to show the nonequivalent carbon atoms in these two examples.



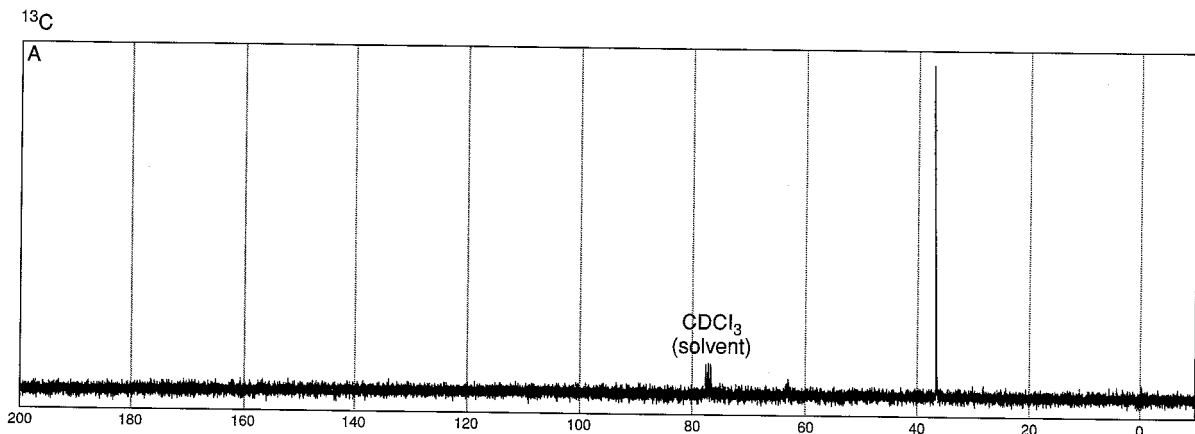
- *3. Following are proton-decoupled ^{13}C spectra for three isomeric alcohols with the formula $\text{C}_4\text{H}_{10}\text{O}$. A DEPT or an off-resonance analysis yields the multiplicities shown; **s** = singlet, **d** = doublet, **t** = triplet, and **q** = quartet. Identify the alcohol responsible for each spectrum, and assign each peak to an appropriate carbon atom or atoms.



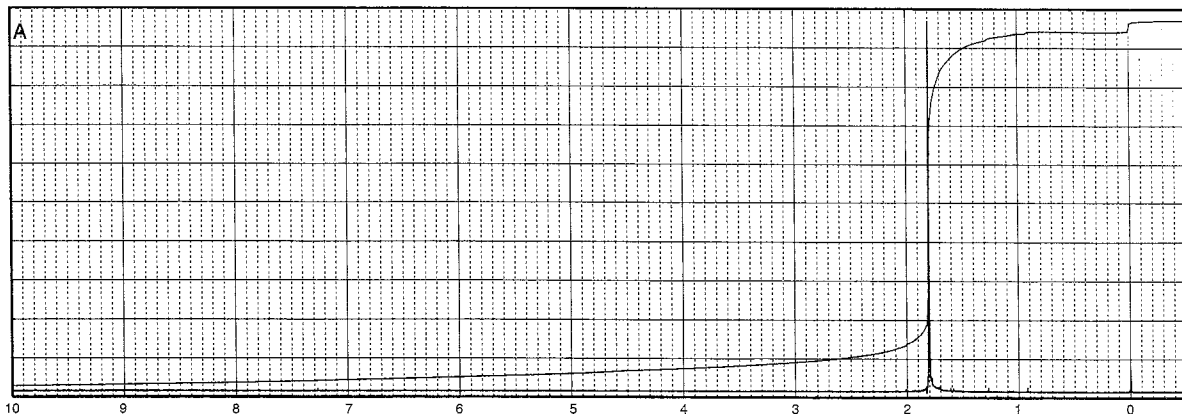
- *4. The following spectrum is of an ester with formula $C_5H_8O_2$. Multiplicities are indicated. Draw the structure of the compound, and assign each peak.



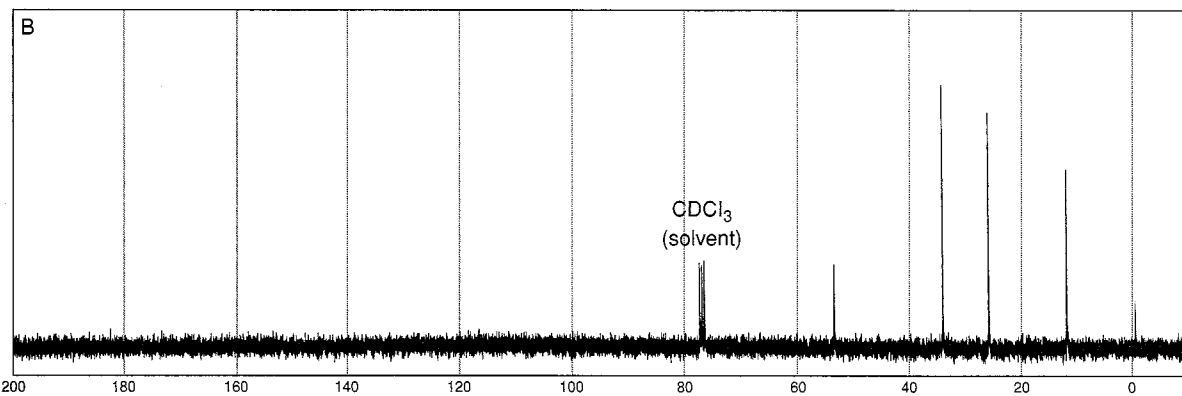
- *5. Following are the 1H and ^{13}C spectra for each of four isomeric bromoalkanes with formula C_4H_9Br . Assign a structure to each pair of spectra.



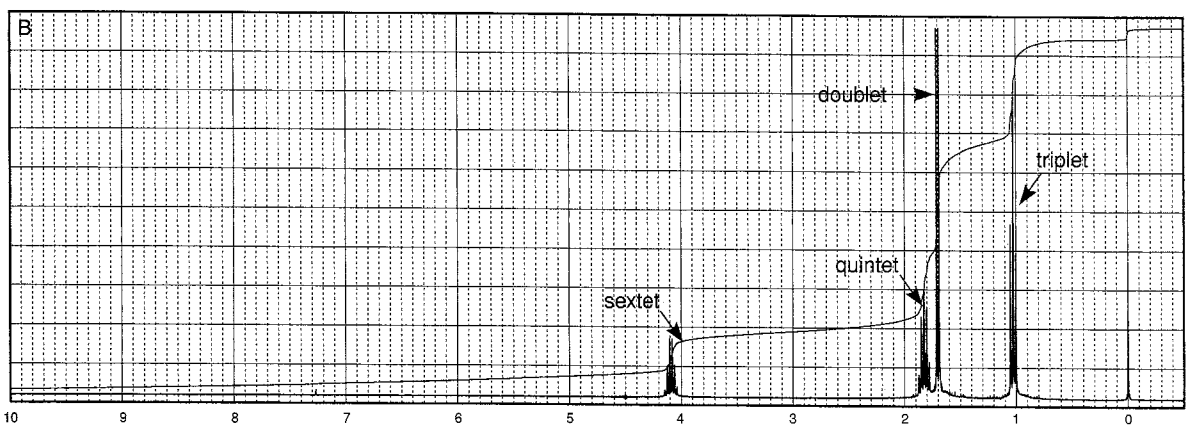
^1H

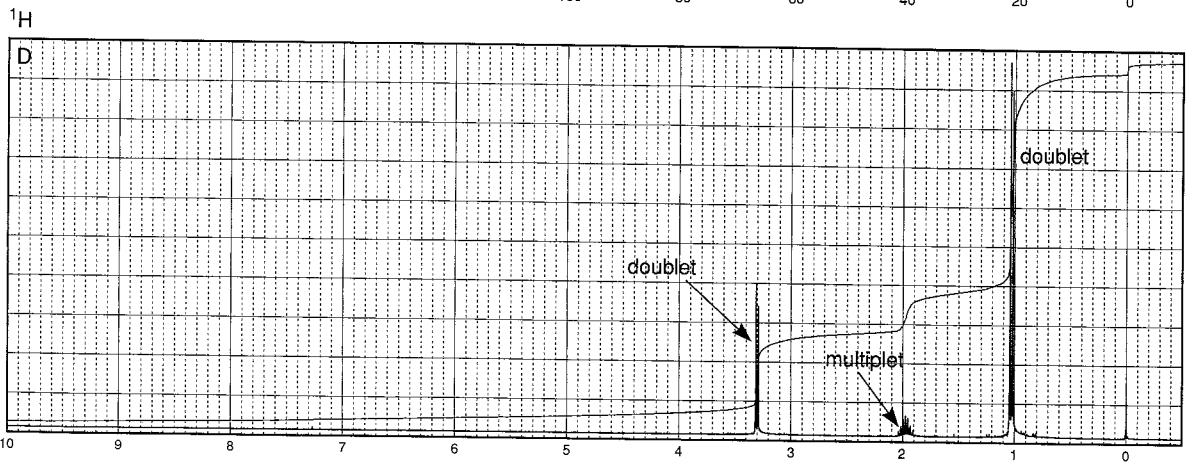
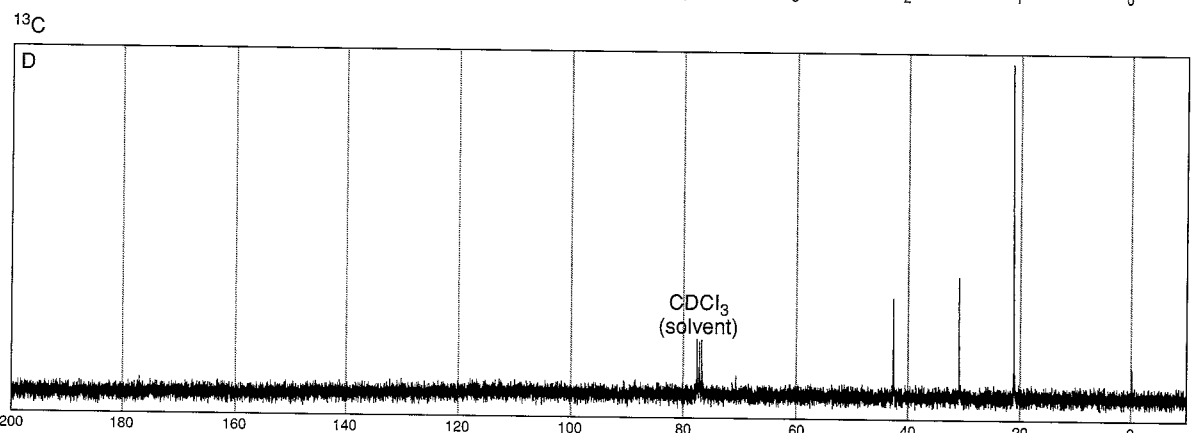
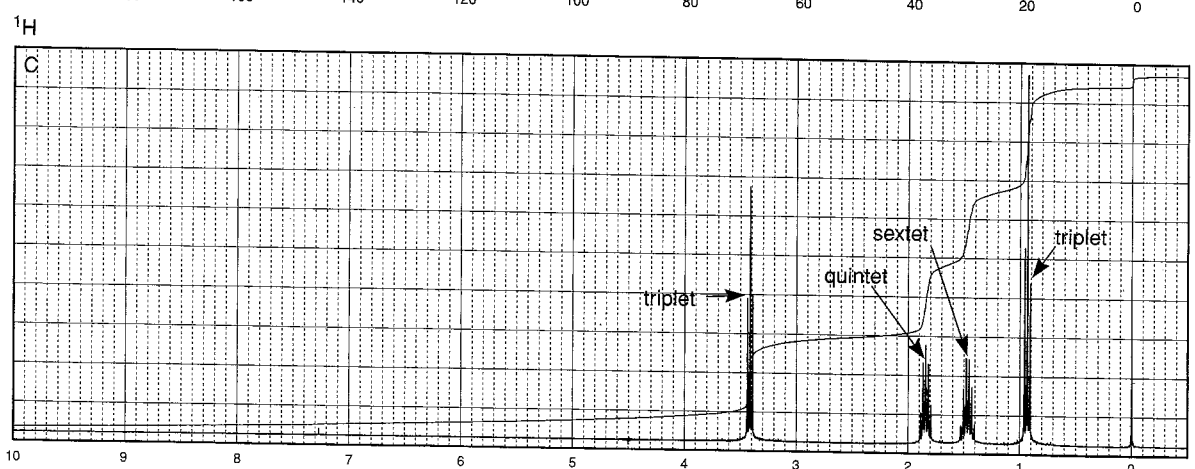
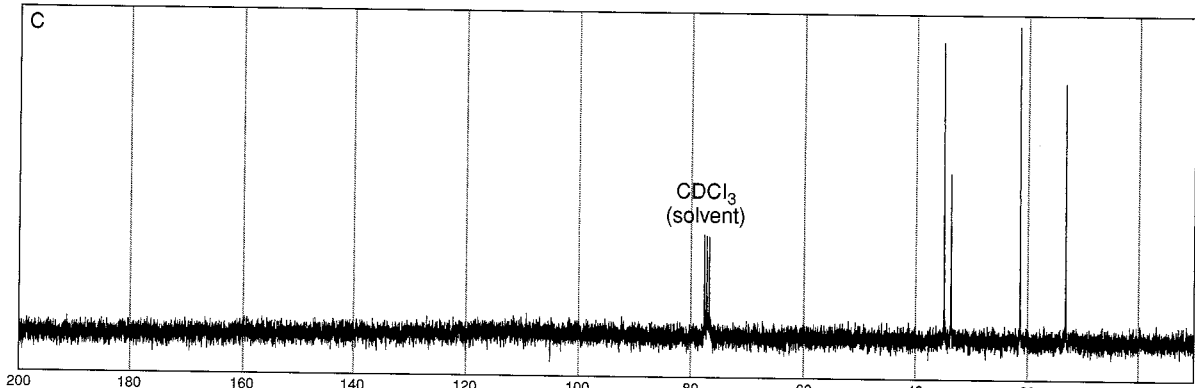


^{13}C

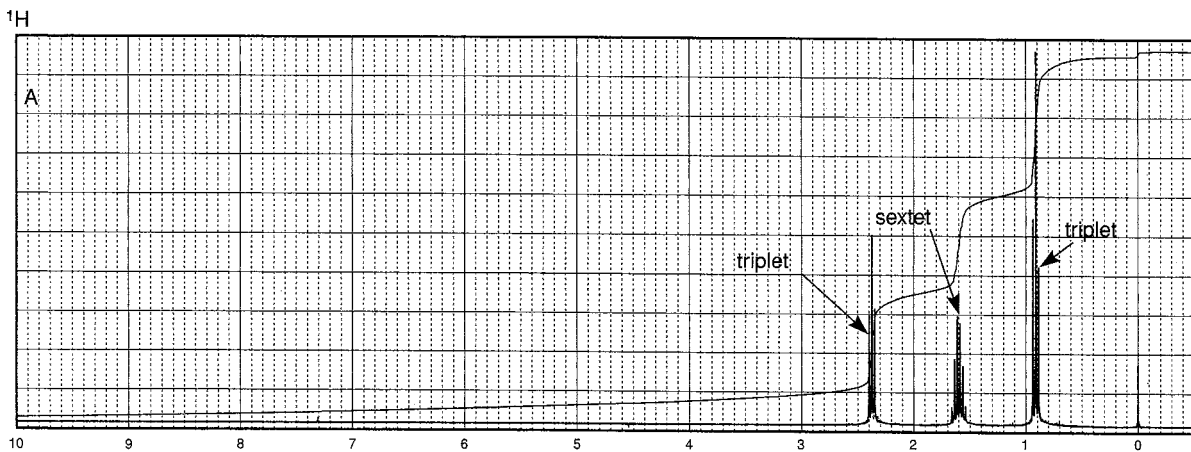
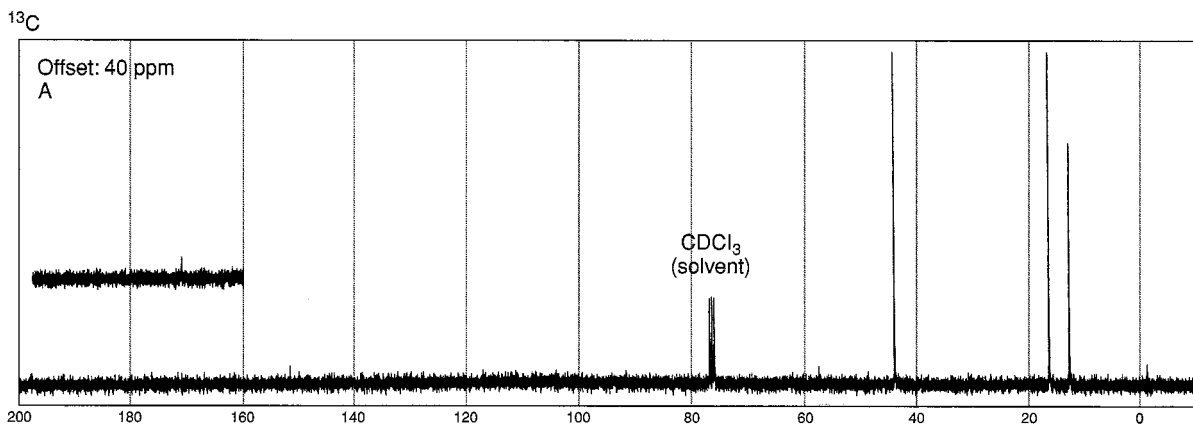


^1H

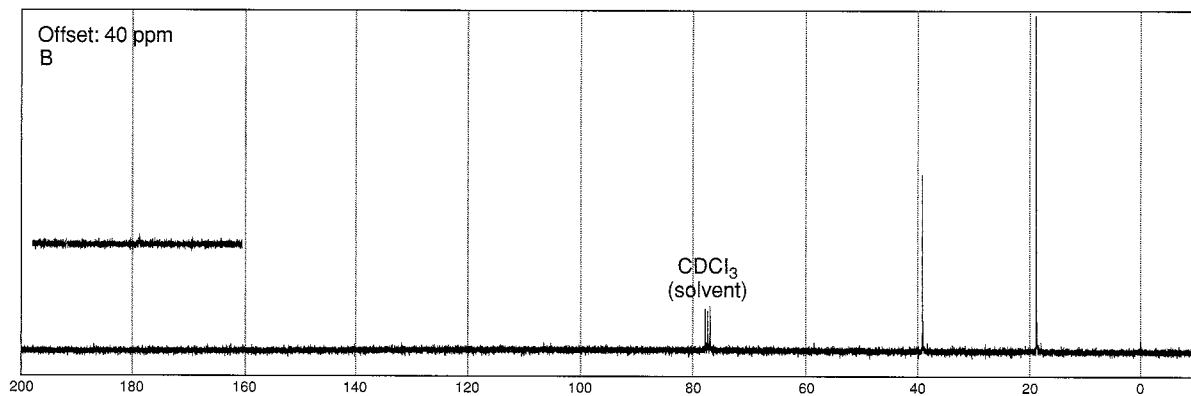




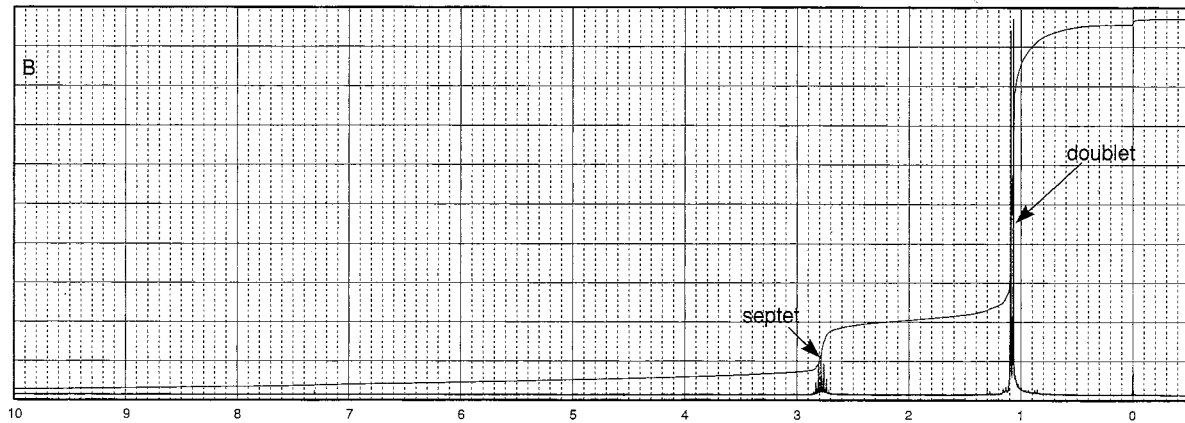
- *6. Following are the ^1H and ^{13}C spectra for each of three isomeric ketones with formula $\text{C}_7\text{H}_{14}\text{O}$. Assign a structure to each pair of spectra.

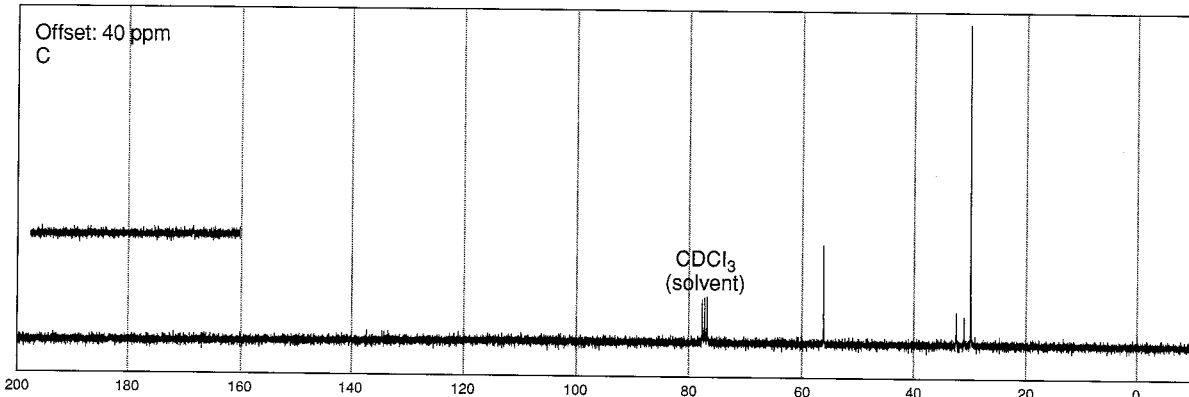
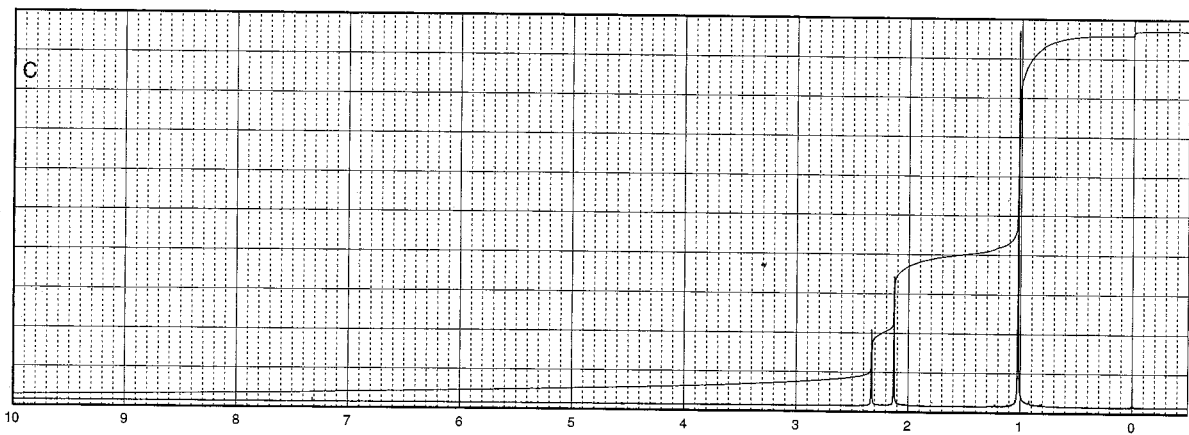


^{13}C



^1H

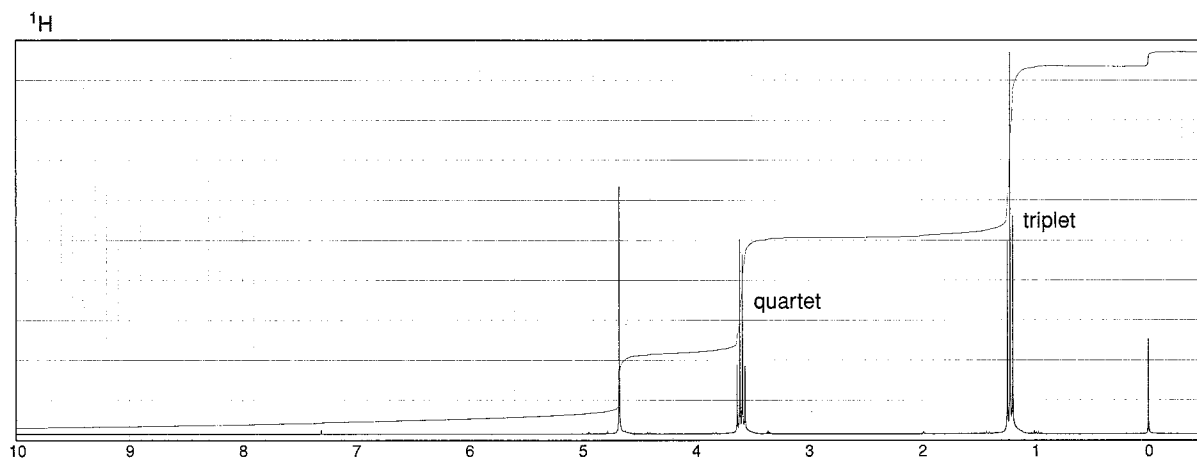


^{13}C  ^1H 

7. The proton NMR spectrum for a compound with formula C_8H_{18} shows only one peak at 0.86 ppm. The carbon-13 NMR spectrum has two peaks, a large one at 26 ppm and a small one at 35 ppm. Draw the structure of this compound.

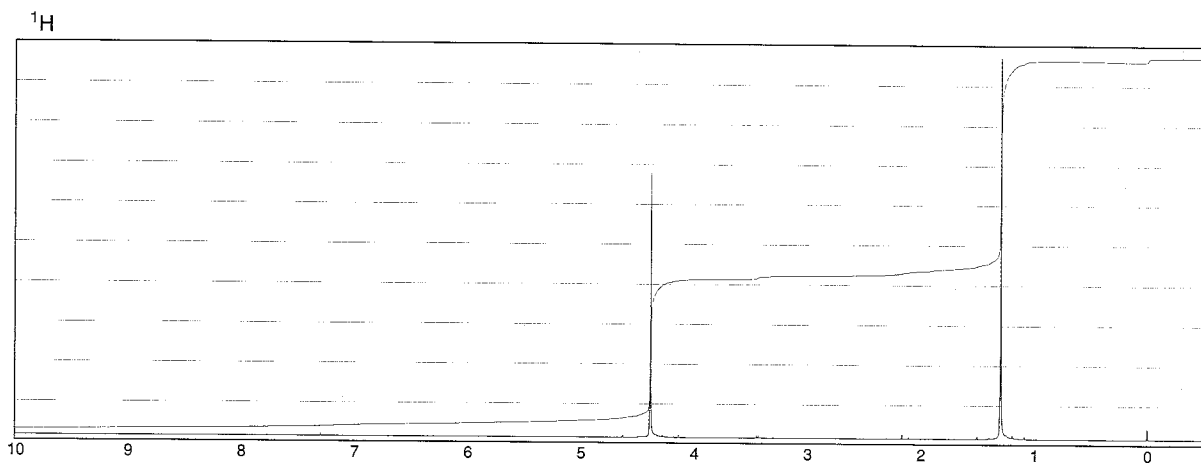
8. The proton NMR spectrum for a compound with formula $C_5H_{12}O_2$ is shown below. The normal carbon-13 NMR spectrum has three peaks. The DEPT-135 and DEPT-90 spectral results are tabulated. Draw the structure of this compound.

Normal Carbon	DEPT-135	DEPT-90
15 ppm	Positive	No peak
63	Negative	No peak
95	Negative	No peak



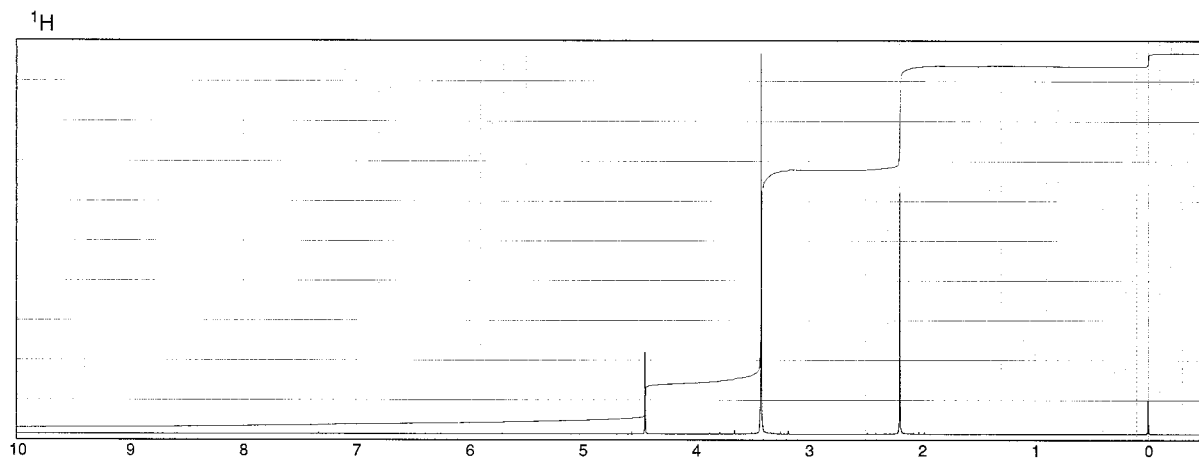
9. The proton NMR spectrum for a compound with formula $C_5H_{10}O$ is shown below. The normal carbon-13 NMR spectrum has three peaks. The DEPT-135 and DEPT-90 spectral results are tabulated. Draw the structure of this compound.

Normal Carbon	DEPT-135	DEPT-90
26 ppm	Positive	No peak
36	No peak	No peak
84	Negative	No peak



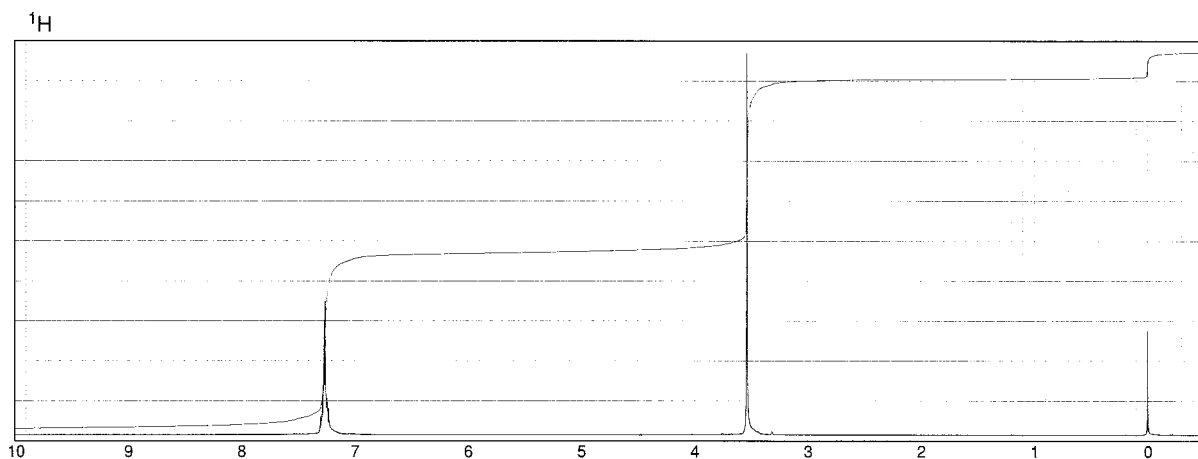
10. The proton NMR spectrum for a compound with formula $C_5H_{10}O_3$ is shown below. The normal carbon-13 NMR spectrum has four peaks. The infrared spectrum has a strong band at 1728 cm^{-1} . The DEPT-135 and DEPT-90 spectral results are tabulated. Draw the structure of this compound.

Normal Carbon	DEPT-135	DEPT-90
25 ppm	Positive	No peak
55	Positive	No peak
104	Positive	Positive
204	No peak	No peak



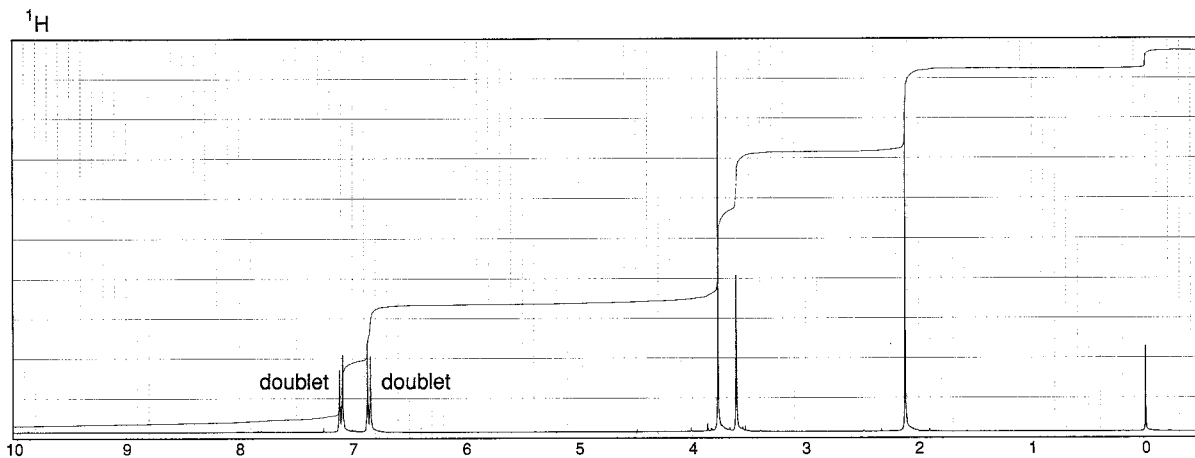
11. The proton NMR spectrum for a compound with formula C_9H_8O is shown below. The normal carbon-13 NMR spectrum has five peaks. The infrared spectrum has a strong band at 1746 cm^{-1} . The DEPT-135 and DEPT-90 spectral results are tabulated. Draw the structure of this compound.

Normal Carbon	DEPT-135	DEPT-90
44 ppm	Negative	No peak
125	Positive	Positive
127	Positive	Positive
138	No peak	No peak
215	No peak	No peak



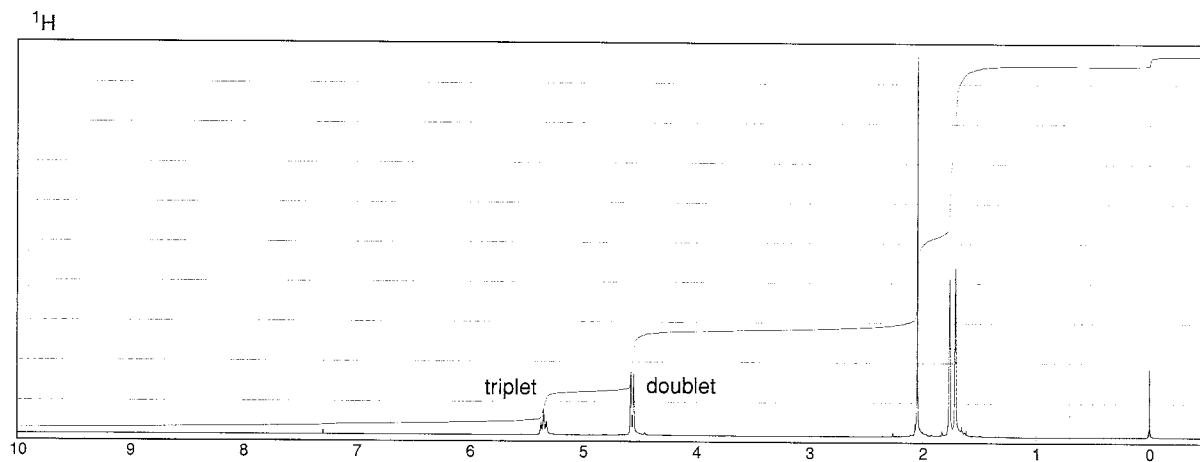
12. The proton NMR spectrum for a compound with formula $C_{10}H_{12}O_2$ is shown below. The infrared spectrum has a strong band at 1711 cm^{-1} . The normal carbon-13 NMR spectral results are tabulated along with the DEPT-135 and DEPT-90 information. Draw the structure of this compound.

Normal Carbon	DEPT-135	DEPT-90
29 ppm	Positive	No peak
50	Negative	No peak
55	Positive	No peak
114	Positive	Positive
126	No peak	No peak
130	Positive	Positive
159	No peak	No peak
207	No peak	No peak



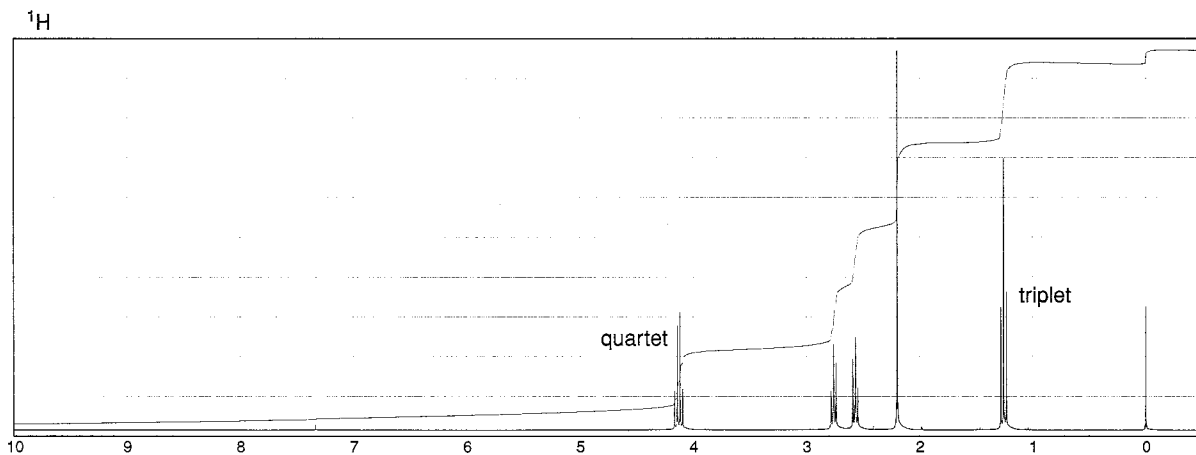
13. The proton NMR spectrum of a compound with formula $C_7H_{12}O_2$ is shown. The infrared spectrum displays a strong band at 1738 cm^{-1} and a weak band at 1689 cm^{-1} . The normal carbon-13 and the DEPT experimental results are tabulated. Draw the structure of this compound.

Normal Carbon	DEPT-135	DEPT-90
18 ppm	Positive	No peak
21	Positive	No peak
26	Positive	No peak
61	Negative	No peak
119	Positive	Positive
139	No peak	No peak
171	No peak	No peak



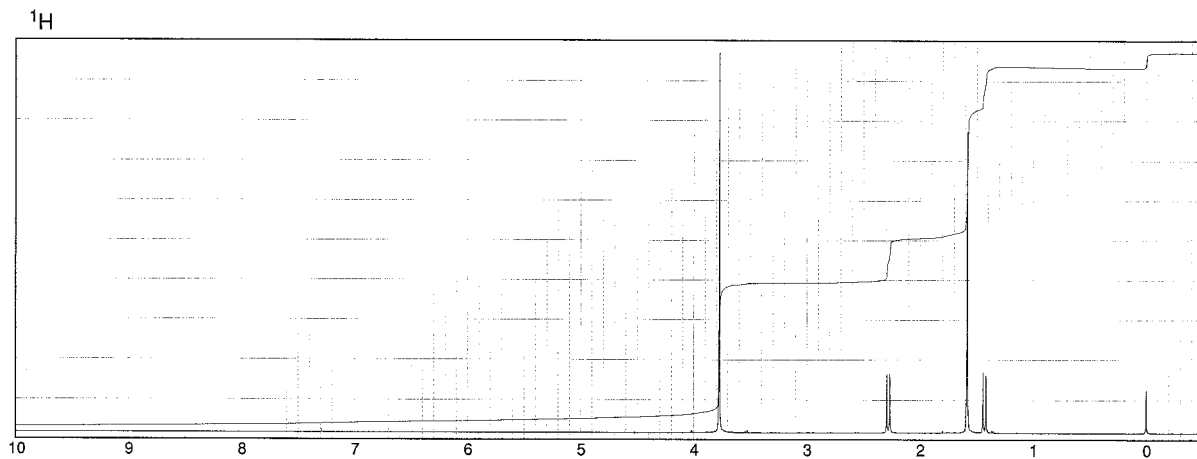
14. The proton NMR spectrum of a compound with formula $C_7H_{12}O_3$ is shown. The coupling constant for the triplet at 1.25 ppm is of the same magnitude as the one for the quartet at 4.15 ppm. The pair of distorted triplets at 2.56 and 2.75 ppm are coupled to each other. The infrared spectrum displays strong bands at 1720 and 1738 cm^{-1} . The normal carbon-13 and the DEPT experimental results are tabulated. Draw the structure of this compound.

Normal Carbon	DEPT-135	DEPT-90
14 ppm	Positive	No peak
28	Negative	No peak
30	Positive	No peak
38	Negative	No peak
61	Negative	No peak
173	No peak	No peak
207	No peak	No peak



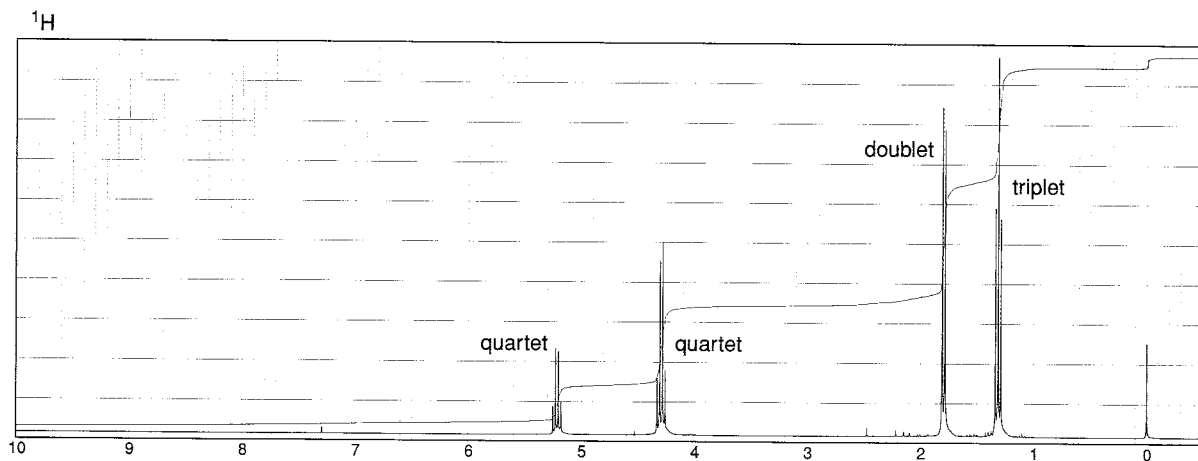
15. The proton NMR spectrum is shown for a compound with formula $C_6H_8Cl_2O_2$. The two chlorine atoms are attached to the same carbon atom. The infrared spectrum displays a strong band 1739 cm^{-1} . The normal carbon-13 and the DEPT experimental results are tabulated. Draw the structure of this compound.

Normal Carbon	DEPT-135	DEPT-90
18 ppm	Positive	No peak
31	Negative	No peak
35	No peak	No peak
53	Positive	No peak
63	No peak	No peak
170	No peak	No peak

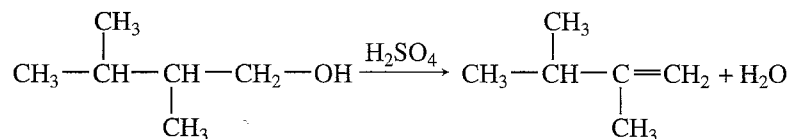


16. The proton NMR spectrum is shown for a compound with formula $C_5H_9NO_4$. The infrared spectrum displays strong bands at 1750 and 1562 cm^{-1} and a medium intensity band at 1320 cm^{-1} . The normal carbon-13 and the DEPT experimental results are tabulated. Draw the structure of this compound.

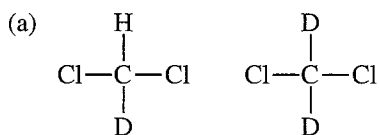
Normal Carbon	DEPT-135	DEPT-90
14 ppm	Positive	No peak
16	Positive	No peak
63	Negative	No peak
83	Positive	Positive
165	No peak	No peak



- *17. The following alcohol undergoes elimination in the presence of concentrated sulfuric acid, but the product shown is not its chief product. Instead, another isomeric six-carbon alkene forms. This product shows a large peak at 20.4 ppm and a smaller one at 123.4 ppm in its proton-decoupled ^{13}C NMR spectrum. Draw the structure of the product, and interpret the spectrum. Outline a mechanism for the formation of the product that possesses this spectrum.

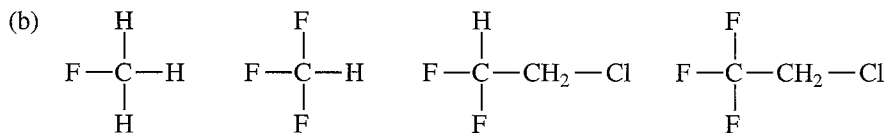


- *18. Predict the appearances of the proton-decoupled ^{13}C spectra for the following compounds.



$$I = 1$$

$$J_{\text{CD}} \cong 20\text{--}30 \text{ Hz (one bond)}$$



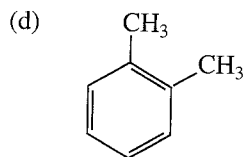
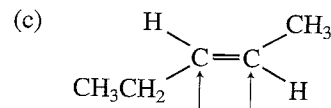
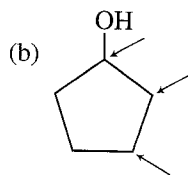
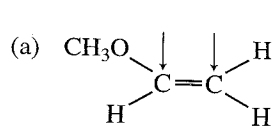
$$I = \frac{1}{2}$$

$$J_{\text{CF}} > 180 \text{ Hz (one bond)}$$

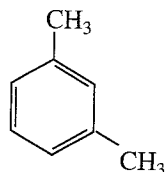
$$J_{\text{CF}} \cong 40 \text{ Hz (two bonds)}$$

- *19. Figure 4.14 (page 188) is the ^{13}C NMR spectrum of toluene. We indicated in Section 4.12 that it was difficult to assign the **c** and **d** carbons to peaks in this spectrum. Using Table 7 in Appendix 8, calculate the expected chemical shifts of all the carbons in toluene, and assign all of the peaks.

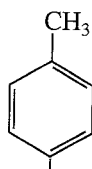
*20. Using the tables in Appendix 8, calculate the expected carbon-13 chemical shifts for the indicated carbon atoms in the following compounds.



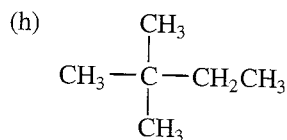
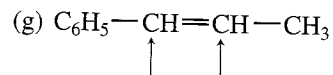
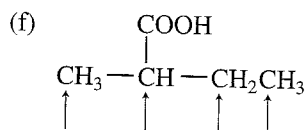
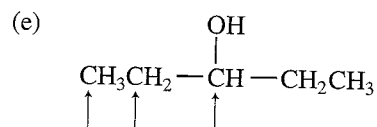
All



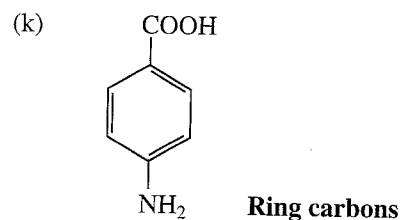
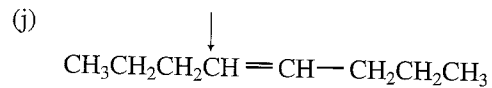
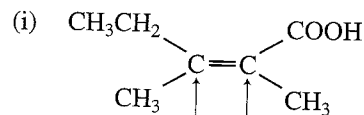
All



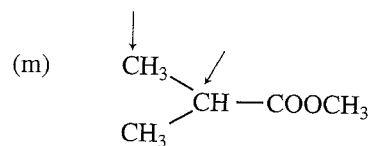
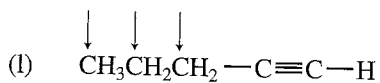
All

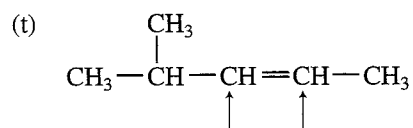
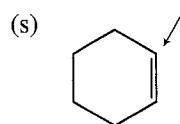
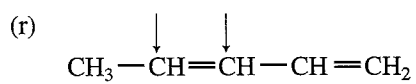
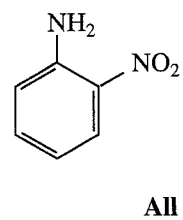
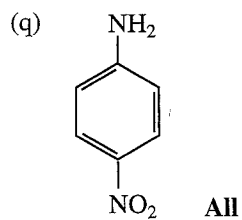
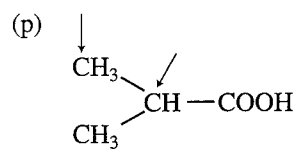
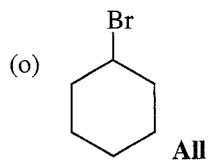
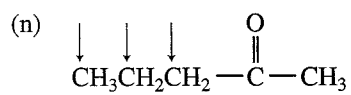


All



Ring carbons





REFERENCES

Textbooks

- Friebolin, H., *Basic One- and Two-Dimensional NMR Spectroscopy*, 2nd ed., VCH Publishers, New York, 1993.
- Gunther, H., *NMR Spectroscopy*, 2nd ed., John Wiley and Sons, New York, 1995.
- Levy, G. C., *Topics in Carbon-13 Spectroscopy*, John Wiley and Sons, New York, 1984.
- Levy, G. C., R. L. Lichter, and G. L. Nelson, *Carbon-13 Nuclear Magnetic Resonance Spectroscopy*, 2d ed., John Wiley and Sons, New York, 1980.
- Levy, G. C., and G. L. Nelson, *Carbon-13 Nuclear Magnetic Resonance for Organic Chemists*, John Wiley and Sons, New York, 1979.
- Macomber, R. S., *NMR Spectroscopy—Essential Theory and Practice*, College Outline Series, Harcourt, Brace Jovanovich, New York, 1988.
- Macomber, R. S., *A Complete Introduction to Modern NMR Spectroscopy*, John Wiley and Sons, New York, 1997.
- Sanders, J. K. M., and B. K. Hunter, *Modern NMR Spectroscopy—A Guide for Chemists*, 2d ed., Oxford University Press, Oxford, England, 1993.
- Silverstein, R. M., and F. X. Webster, *Spectrometric Identification of Organic Compounds*, 6th ed., John Wiley and Sons, New York, 1998.
- Yoder, C. H., and C. D. Schaeffer, *Introduction to Multinuclear NMR*, Benjamin-Cummings, Menlo Park, CA, 1987.

Compilations of Spectra

- Ault, A., and M. R. Ault, *A Handy and Systematic Catalog of NMR Spectra*, 60 MHz with some 270 MHz, University Science Books, Mill Valley, CA, 1980.
- Fuchs, P. L., *Carbon-13 NMR Based Organic Spectral Problems*, 25 MHz, John Wiley and Sons, New York, 1979.
- Johnson, L. F., and W. C. Jankowski, *Carbon-13 NMR Spectra: A Collection of Assigned, Coded, and Indexed Spectra*, 25 MHz, Wiley-Interscience, New York, 1972.
- Pouchert, C. J., and J. Behnke, *The Aldrich Library of ¹³C and ¹H FT-NMR Spectra*, 75 and 300 MHz, Aldrich Chemical Company, Milwaukee, WI, 1993.
- Pretsch, E., T. Clerc, J. Seibl, and W. Simon, *Tables of Spectral Data for Structure Determination of Organic Compounds*, 2nd ed., Springer-Verlag, Berlin and New York, 1989. Translated from the German by K. Biemann.

Computer Programs that Teach Carbon-13 NMR Spectroscopy

- Clough, F. W., "Introduction to Spectroscopy," Version 2.0 for MS-DOS and Macintosh, Trinity Software, 607 Tenney Mtn. Highway, Suite 215, Plymouth, NH, 03264, www.trinitysoftware.com.
- Schatz, P. F., "Spectrabook I and II," MS-DOS Version, and "Spectradeck I and II," Macintosh Version, Falcon Software, One Hollis Street, Wellesley, MA, 02482, www.falconssoftware.com.

Computer Estimation of Carbon-13 Chemical Shifts

- "C-13 NMR Estimate," IBM PC/Windows, Software for Science, 2525 N. Elston Ave., Chicago, IL 60647.
- "¹³C NMR Estimation," CS ChemDraw Ultra, Cambridge SoftCorp., 100 Cambridge Park Drive, Cambridge, MA 02140.
- "Carbon 13 NMR Shift Prediction Module" requires ChemWindow (IBM PC) or ChemIntosh (Macintosh), SoftShell International, Ltd., 715 Horizon Drive, Grand Junction, CO 81506.
- "HyperNMR," IBM PC/Windows, Hypercube, Inc., 419 Phillip Street, Waterloo, Ontario, Canada N2L 3X2.
- "TurboNMR," Silicon Graphics Computers, Biosym Technologies, Inc., 4 Century Drive, Parsippany, NJ 07054.

Web sites

- <http://www.aist.go.jp/RIODB/SDBS/menu-e.html>
Integrated Spectral DataBase System for Organic Compounds, National Institute of Materials and Chemical Research, Tsukuba, Ibaraki 305-8565, Japan. This database includes infrared, mass spectra, and NMR data (proton and carbon-13) for a number of compounds.
- <http://www.chem.ucla.edu/~webnmr>
UCLA Department of Chemistry and Biochemistry, in connection with Cambridge University Isotope Laboratories, maintains a website, WebSpectra, that provides NMR and IR spectroscopy problems for students to interpret. They provide links to other sites with problems for students to solve.
- <http://www.nd.edu/~smithgrp/structure/workbook.html>
Combined structure problems provided by the Smith group at Notre Dame University.